& Kurose, H. (2008) P2Y6 receptor-Galpha12/13 signalling in cardiomyocytes triggers pressure overload-induced cardiac fibrosis. *EMBO J.* **27**, 3104–3115.

Nishikimi, T., Maeda, N. & Matsuoka, H. (2006) The role of natriuretic peptides in cardioprotection. *Cardiovasc. Res.* **69**, 318–328.

Rosenkranz, S. (2004) TGF-beta1 and angiotensin networking in cardiac remodeling. *Cardiovasc. Res.* **63**, 423–432.

Stamenkovic, I. (2003) Extracellular matrix remodelling: the role of matrix metalloproteinases. *J. Pathol.* **200**, 448–464.

Virag, J.A., Rolle, M.L., Reece, J., Hardouin, S., Feigl, E.O. & Murry, C.E. (2007) Fibroblast growth factor-2 regulates myocardial infarct repair: effects on cell proliferation, scar contraction, and ventricular function. *Am. J. Pathol.* **171**, 1431–1440.

Weber, K.T. & Brilla, C.G. (1991) Pathological hypertrophy and cardiac interstitium. Fibrosis and renin-angiotensin-aldosterone system. *Circulation* **83**, 1849–1865.

Xu, Q., Ming, Z., Dart, A.M. & Du, X.J. (2007) Optimizing dosage of ketamine and xylazine in murine echocardiography. *Clin. Exp. Pharmacol. Physiol.* **34**, 499–507.

Received: 4 February 2013
Accepted: 10 March 2013

Hum Genet (2013) 132:783–792
DOI 10.1007/s00439-013-1294-3

ORIGINAL INVESTIGATION

Genome-wide scan revealed that polymorphisms in the *PNPLA3*, *SAMM50*, and *PARVB* genes are associated with development and progression of nonalcoholic fatty liver disease in Japan

Takuya Kitamoto · Aya Kitamoto · Masato Yoneda · Hideyuki Hyogo · Hidenori Ochi · Takahiro Nakamura · Hajime Teranishi · Seiho Mizusawa · Takato Ueno · Kazuaki Chayama · Atsushi Nakajima · Kazuwa Nakao · Akihiro Sekine · Kikuko Hotta

Received: 14 January 2013 / Accepted: 17 March 2013 / Published online: 28 March 2013

Abstract We examined the genetic background of nonalcoholic fatty liver disease (NAFLD) in the Japanese population, by performing a genome-wide association study (GWAS). For GWAS, 392 Japanese NAFLD subjects and 934 control individuals were analyzed. For replication studies, 172 NAFLD and 1,012 control subjects were monitored. After quality control, 261,540 single-nucleotide polymorphisms (SNPs) in autosomal chromosomes were analyzed using a trend test. Association analysis was also performed using multiple logistic regression analysis using genotypes, age, gender and body mass index (BMI) as independent variables. Multiple linear regression analyses were performed to evaluate allelic effect of significant SNPs on biochemical traits and histological parameters adjusted by age, gender, and BMI. Rs738409 in the *PNPLA3* gene was most strongly associated with NAFLD after adjustment ($P = 6.8 \times 10^{-14}$, OR = 2.05). Rs2896019, and rs381062 in the *PNPLA3* gene, rs738491, rs3761472, and rs2143571 in the *SAMM50* gene, rs6006473, rs5764455, and rs6006611 in the *PARVB* gene had also significant *P* values ($<2.0 \times 10^{-10}$) and high odds ratios (1.84–2.02). These SNPs were found to be in the same linkage disequilibrium block and were associated with decreased serum triglycerides and increased aspartate aminotransferase (AST) and alanine aminotransferase (ALT) in NAFLD patients. These SNPs were associated with steatosis grade and NAFLD activity score (NAS). Rs738409, rs2896019, rs738491, rs6006473, rs5764455, and rs6006611 were associated with fibrosis. Polymorphisms in the *SAMM50* and *PARVB* genes in addition to those in the *PNPLA3* gene were observed to be associated with the development and progression of NAFLD.

Introduction

Nonalcoholic fatty liver disease (NAFLD) is now recognized as an important health concern (Angulo 2002; Farrell

Electronic supplementary material The online version of this article (doi:10.1007/s00439-013-1294-3) contains supplementary material, which is available to authorized users.

T. Kitamoto · A. Kitamoto · K. Nakao · A. Sekine · K. Hotta (✉)
EBM Research Center, Kyoto University Graduate School of Medicine, Yoshida-Konoecho, Sakyo-ku, Kyoto 606-8501, Japan
e-mail: kikukoh@kuhp.kyoto-u.ac.jp

M. Yoneda · A. Nakajima
Division of Gastroenterology, Yokohama City University Graduate School of Medicine, Yokohama, Japan

H. Hyogo · H. Ochi · K. Chayama
Division of Frontier Medical Science, Department of Medicine and Molecular Science, Programs for Biomedical Research, Graduate School of Biomedical Sciences, Hiroshima University, Hiroshima, Japan

T. Nakamura
Laboratory for Mathematics, National Defense Medical College, Tokorozawa, Japan

H. Teranishi · S. Mizusawa
Center for Genomic Medicine, Unit of Genome Informatics, Kyoto University Graduate School of Medicine, Kyoto, Japan

T. Ueno
Research Center for Innovative Cancer Therapy, Kurume University, Kurume, Japan

K. Nakao
Department of Medicine and Clinical Science, Kyoto University Graduate School of Medicine, Kyoto, Japan

2003). NAFLD has a broad spectrum of effects, including simple steatosis, nonalcoholic steatohepatitis (NASH), fibrosis/cirrhosis, and hepatocellular carcinoma. Excess fat accumulation in the liver is observed in 20–30 % of the population in American and European countries, where NASH is associated with approximately 1–3 % of the population (Ludwig et al. 1980). NAFLD is now considered to be a part of metabolic syndrome (Marchesini et al. 2001; Stefan et al. 2008). Genetic as well as environmental factors are important in the development of NAFLD (Wilfred de Alwis and Day 2008).

Single-nucleotide polymorphisms (SNPs) are useful tools for identifying genetic factors and have been intensively investigated for various common diseases. We previously reported that variations in peroxisome proliferator-activated receptor γ coactivator 1α (*PPARGC1A*), angiotensin II type 1 receptor (*ATGR1*), and nitric oxide synthase 2 (inducible) (*NOS2*) genes are associated with NAFLD in Japanese individuals (Yoneda et al. 2008, 2009a, b).

Genome-wide association studies (GWASs) have revealed that SNPs in the patatin-like phospholipase domain containing 3 (*PNPLA3*) and other genes influence NAFLD and liver enzyme levels in the plasma (Romeo et al. 2008; Chalasani et al. 2010; Speliotes et al. 2011; Kawaguchi et al. 2012). We previously reported that the risk allele (G-allele) of *PNPLA3* rs738409 is strongly associated with NAFLD as well as with increases in aspartate transaminase (AST), alanine transaminase (ALT), ferritin levels, and fibrosis stage in the patients with NAFLD in the Japanese population (Hotta et al. 2010).

To elucidate the detailed genetic background of NAFLD in the Japanese population, we performed genome-wide analysis for NAFLD.

Materials and methods

Subjects

For GWAS, 392 Japanese patients with NAFLD (NAFLD-1; 345 with NASH and 47 with simple steatosis) were enrolled. Genome-wide scan data for 934 general Japanese control subjects (control-1) described in the JSNP database (IMS-JST: Institute of Medical Science-Japan Science and Technology Agency Japanese SNP database, http://snp.ims.u-tokyo.ac.jp/) were used for GWAS. For the replication study, 172 patients with NAFLD (NAFLD-2; 97 with NASH, 4 with simple steatosis, and 71 with NAFLD) and 1012 control subjects (control-2) were analyzed. Control-2 subjects included Japanese volunteers who had undergone medical examination for common disease screening. All the NAFLD-1 and 101 NAFLD-2 patients underwent liver biopsy. Computed tomography (CT) or magnetic resonance imaging (MRI) was performed on 71 NAFLD-2 patients. Patients with the following diseases were excluded from the study: viral hepatitis (hepatitis B and C, Epstein–Barr virus infection), autoimmune hepatitis, primary biliary cirrhosis, sclerosing cholangitis, hemochromatosis, α_1-antitrypsin deficiency, Wilson's disease, drug-induced hepatitis, and alcoholic hepatitis (present or past daily consumption of more than 20 g alcohol per day). None of the patients showed clinical evidence of hepatic decompensation such as hepatic encephalopathy, ascites, variceal bleeding, or a serum bilirubin level greater than twofold the normal upper limit.

Liver biopsy tissues were stained with hematoxylin and eosin, reticulin, and Masson's trichrome stain. Histological criterion for NAFLD diagnosis is macrovesicular fatty change in hepatocytes with displacement of the nucleus toward the cell edge (Sanyal 2002). When more than 5 % of hepatocytes are affected by macrovesicular steatosis, patients are diagnosed as having either steatosis or NASH. The minimal criteria for the diagnosis of NASH includes the presence of >5 % macrovesicular steatosis, inflammation, and liver cell ballooning, typically with predominantly centrilobular (acinar zone 3) distribution (Matteoni et al. 1999; Teli et al. 1995). Steatosis degree was graded as follows based on the percentage of hepatocytes containing macrovesicular fat droplets: grade 0, no steatosis; grade 1, <33 % hepatocytes containing macrovesicular fat droplets; grade 2, 33–66 % of hepatocytes containing macrovesicular fat droplets; and grade 3, >66 % of hepatocytes containing macrovesicular fat droplets (Brunt 2001). The activity of hepatitis (necroinflammatory grade) was also determined on the basis of the composite NAFLD activity score (NAS) as described by Kleiner et al. (2005). NAS is the unweighted sum of the scores for steatosis, lobular inflammation, and hepatocellular ballooning, and ranges from 0 to 8. Fibrosis severity was scored according to the method of Brunt (2001) and was expressed on a 4-point scale, as follows: 0, none; 1, perivenular and/or perisinusoidal fibrosis in zone 3; 2, combined pericellular portal fibrosis; 3, septal/bridging fibrosis; 4, cirrhosis.

Entire study was conducted in accordance with the guidelines of the Declaration of Helsinki. Written informed consent was obtained from each subject, and the protocol was approved by the ethics committee of Kyoto University, Yokohama City University, Hiroshima University, and Kurume University.

Clinical and laboratory evaluation

The weight and height of patients were measured using a calibrated scale after removing shoes and heavy clothing, if present. Venous blood samples were obtained from subjects after overnight fasting (12 h) to measure plasma

glucose, hemoglobin A1c (HbA1c), total cholesterol, high-density lipoprotein (HDL) cholesterol, triglycerides, serum AST, ALT, iron, ferritin, hyaluronic acid, and type IV collagen 7S. All the laboratory biochemical parameters were measured using conventional methods.

DNA preparation, genome-wide genotyping and quality control

Genomic DNA was extracted using Genomix (Talent Srl, Trieste, Italy) for blood samples collected from each subject. Genome scans were conducted for NAFLD-1 patients using the Human660 W-Quad BeadChip ($n = 104$) or the HumanOmniExpress BeadChip ($n = 288$; Illumina, Inc., San Diego, CA, USA). Genome scan data from control-1 ($n = 934$) were genotyped using the Illumina HumanHap550 BeadChip and 515,286 SNPs in the autosomal chromosome were available in the JSNP database. A total of 295,887 common SNPs in the autosomal chromosomes were determined among 3 BeadChips. Individual call rates were all >0.99 in the patients and the control group. A total of 31,177 SNPs with minor allele frequency (<0.01), 901 SNPs with a lower success rate (<0.95), and 2,269 SNPs with distorted Hardy–Weinberg equilibrium ($P < 0.001$) were excluded; thus, 261,540 SNPs were subjected to case–control association analysis. Using phase II and III HapMap JPT, HCB and CEU data (http://hapmap.ncbi.nlm.nih.gov/), we confirmed that NAFLD-1 subjects in this study were derived from the Japanese population using multi-dimensional scaling (MDS) analysis (Supplementary Fig. 1). The number of alleles that shared identity-by-descent (PI_HAT) was calculated, and it was found that the PI_HAT value was less than 0.05 for the NAFLD-1 patients.

For the replication study, Invader probes (Third Wave Technologies, Madison, WI, USA) were constructed for 56 SNPs with P values less than 5.0×10^{-5}. SNPs were genotyped for NAFLD-2 and control-2 using Invader assays as previously described (Ohnishi et al. 2001). The success rates of the Invader assays were >99.0 %. To validate GWAS, NAFLD-1 patients were also genotyped using the Invader assay and SNPs with concordance rate of both genotyping more than 99 % were used for further analysis. Thirteen SNPs showed a lower concordance rate (<0.99) and were excluded from further analysis.

Table 1 Clinical characteristic of the subjects

	GWAS		Replication	
	NAFLD-1 ($n = 392$)	Control-1 ($n = 934$)	NAFLD-2 ($n = 172$)	Control-2 ($n = 1012$)
No. of NASH	345	–	97	–
Men/women	199/193	–	95/77	500/512
Age (year)	49.9 ± 14.8	–	53.5 ± 13.8	53.1 ± 15.3
BMI (kg/m^2)	28.0 ± 5.0	–	27.4 ± 4.6	22.7 ± 3.2
FPG (mg/dL)	118.8 ± 37.3	–	114.8 ± 36.8	98.2 ± 19.0
Hb.A1c (%)	6.4 ± 1.3	–	6.3 ± 1.1	5.5 ± 0.7
T. Chol. (mg/dL)	213.7 ± 41.4	–	205.0 ± 39.6	208.5 ± 36.2
Triglycerides (mg/dL)	172.2 ± 120.6	–	153.3 ± 74.4	110.0 ± 88.5
HDL-C (mg/dL)	52.9 ± 15.7	–	53.8 ± 12.7	62.7 ± 15.5
SBP (mmHg)	127.5 ± 15.0	–	129.6 ± 14.0	124.5 ± 19.1
DBP (mmHg)	78.0 ± 11.7	–	81.1 ± 9.4	76.3 ± 11.6
AST (IU/L)	51.3 ± 31.5	–	47.9 ± 25.4	23.0 ± 10.2
ALT (IU/L)	84.3 ± 60.2	–	75.4 ± 53.6	20.3 ± 11.8
Ferritin (ng/mL)	237.1 ± 225.0	–	229.1 ± 227.3	–
Hyaluronic acid (ng/dL)	44.5 ± 70.2	–	74.8 ± 208.2	–
Type IV collagen 7s (ng/dL)	4.4 ± 1.3	–	6.2 ± 12.8	–
Steatosis grade (1–3)	1.6 ± 0.7	–	1.5 ± 0.8[a]	–
Lobular inflammation (0–3)	1.2 ± 0.8	–	1.5 ± 0.6[a]	–
Hepatocyte ballooning (0–2)	1.1 ± 0.7	–	1.2 ± 0.5[a]	–
NAS (0–8)	4.0 ± 1.7	–	4.2 ± 1.3[a]	–
Fibrosis stage (0–4)	1.6 ± 1.0	–	2.0 ± 1.0[a]	–

AST aspartate transaminase, *ALT* alanine transaminase, *DBP* diastolic blood pressure, *FPG* fasting plasma glucose, *HDL-C* high-density lipoprotein cholesterol, *SBP* systolic blood pressure, *SNP* single-nucleotide polymorphism, *T. Chol.* total cholesterol

[a] $n = 101$

Statistical analysis

A case–control association analysis was performed using the Cochran-Armitage trend test. Combined *P* values were obtained using Fisher's combined probability test. Hardy–Weinberg equilibrium was assessed using the χ^2-test (Nielsen et al. 1998). PI_HAT and MDS analysis were performed using PLINK 1.07 (http://pngu.mgh.harvard.edu/purcell/plink) (Purcell et al. 2007). A Manhattan plot of GWAS and linkage disequilibrium (LD) was drawn using HaploView (Barrett et al. 2005). We categorized the genotypes as 0, 1, or 2 depending on the number of copies of risk alleles present. Multiple linear regression analyses were performed to test the independent effect per allele of each SNP on biochemical traits and histological parameters, accounting for effects of the other variables [i.e., age, gender, and body mass index (BMI)]. BMI, fasting plasma glucose, triglycerides, ferritin, hyaluronic acid, and type IV collagen 7 s values were logarithmically transformed before performing multiple linear regression analysis. Statistical analyses were performed using R software (http://www.r-project.org/).

Results

Genome-wide case–control association studies

We performed GWAS using NAFLD-1 ($n = 392$) and control-1 ($n = 934$). The characteristics of the study samples are presented in Table 1. After quality controls of genotyping results, 261,540 SNPs in autosomal chromosomes were used for case–control association analysis. To assess population stratification, we examined the quantile–quantile *P* value plot (Fig. 1a). A slight inflation in *P* values was observed according to the genomic control method ($\lambda_{GC} = 1.09$). Because we used the JSNP database as a control, we were unable to evaluate population stratification between NAFLD-1 and control-1 subjects. Instead, we confirmed that all the NAFLD-1 subjects were collected from the Japanese population using MDS analysis (Supplementary Fig. 1).

To identify SNPs susceptible to causing NAFLD, we compared NAFLD-1 and control-1 subjects using the trend test. A Manhattan plot showed that one peak located on chromosome 22q13 was significantly associated with NAFLD and that some SNPs were marginally associated with NAFLD (Fig. 1b; Supplementary Fig. 3). To evaluate significant and marginally NAFLD-associated SNPs, we selected 56 SNPs with *P* values less than 5.0×10^{-5}. We performed a replication study of NAFLD-2 ($n = 172$) and control-2 ($n = 1012$) subjects. After the replication study, 12 SNPs remained with *P* values less than 1.0×10^{-5}, and

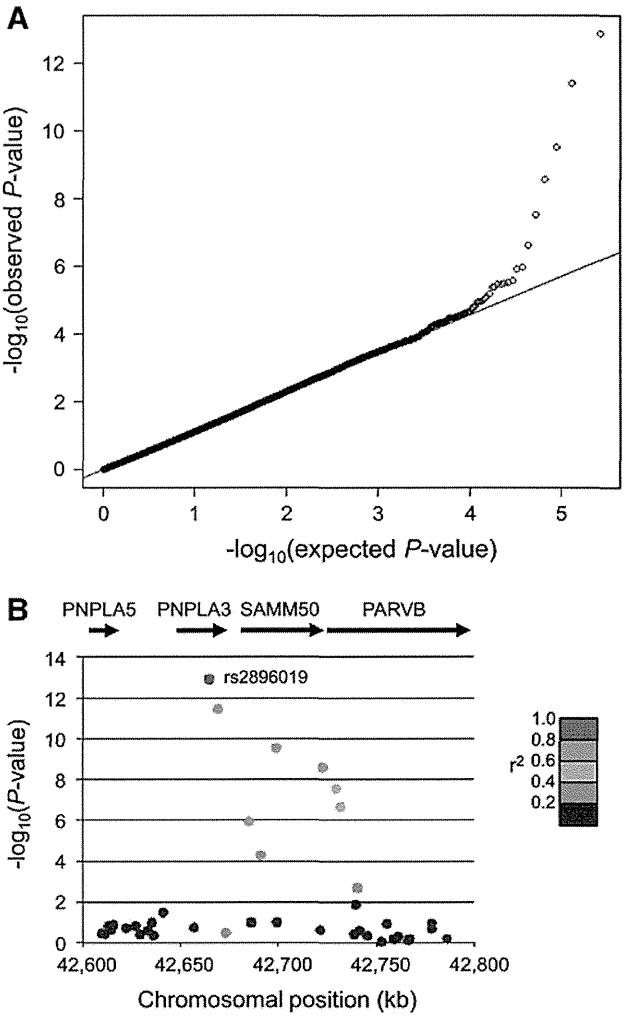

Fig. 1 Quantile–quantile plot for genome-wide association (**a**) and regional plots of genome-wide significant loci (**b**). **a** The $-\log_{10}$ (*P* value) of observed association statistics is shown in *y*-axis, compared with −log10 (*P* value) of the association statistics expected under the null hypothesis of no association in *x*-axis. **b**. SNPs are plotted by their position on the chromosome against their association with NAFLD using GWAS data. The SNPs surrounding the top SNP (rs2896019) are colored to reflect their LD with the top SNP (using pairwise r^2 values from GWAS data of NAFLD-1 and control-1). The positions of genes as well as the direction of transcription are shown above the plots

8 SNPs were significantly associated with NAFLD even when conservative Bonferroni's correction was applied ($P < 1.0 \times 10^{-9}$, Table 2). All the eight SNPs were in the same LD block (Fig. 1b; Supplementary Fig. 2) and located at chromosome 22q13, which was previously reported to be NAFLD-susceptible (Romeo et al. 2008; Speliotes et al. 2011; Kawaguchi et al. 2012; Hotta et al. 2010). NAFLD patients have higher BMI compared with the Japanese general population (Table 1); thus, we performed multiple logistic regression analysis using genotypes, age, gender, and BMI as independent variables, involving

Table 2 List of the SNPs showing combined $P < 1.0 \times 10^{-5}$

dbSNP ID	Chr	BP (Build 36.3)	Nearby genes	Allele ½	GWAS				Replication				Combined *P* value
					Genotype (risk allele frequency)		*P* value	OR (95 % CI)	Genotype (risk allele frequency)		*P* value	OR (95 % CI)	
					NAFLD-1	Control-1			NAFLD-2	Control-2			
rs6691847	1	30,038,239	*PTPRU*	T/C[a]	11/106/275 (0.84)	48/355/531 (0.76)	7.2×10^{-6}	1.63 (1.31–2.03)	8/46/116 (0.82)	47/366/599 (0.77)	0.063	1.32 (0.98–1.77)	7.3×10^{-6}
rs7552722	1	115,722,878	*NGF*	A[a]/G	70/180/142 (0.41)	100/390/444 (0.32)	7.9×10^{-6}	1.49 (1.26–1.78)	22/84/66 (0.37)	124/394/490 (0.32)	0.059	1.27 (1.00–1.61)	7.2×10^{-6}
rs2051090	13	35,352,193	*DCLK1*	A/G[a]	4/108/280 (0.85)	51/328/555 (0.77)	1.6×10^{-6}	1.72 (1.38–2.16)	2/52/118 (0.84)	40/299/669 (0.81)	0.27	1.19 (0.88–1.62)	7.1×10^{-6}
rs2896019	22	42,665,027	*PNPLA3*	T/G[a]	75/155/162 (0.61)	290/453/191 (0.45)	1.3×10^{-13}	1.94 (1.64–2.30)	23/83/66 (0.63)	300/509/202 (0.45)	2.5×10^{-9}	2.02 (1.60–2.56)	1.6×10^{-20}
rs3810622	22	42,669,467	*PNPLA3*	A[a]/G	208/141/43 (0.71)	291/470/172 (0.56)	3.9×10^{-12}	1.90 (1.59–2.27)	92/63/17 (0.72)	314/517/180 (0.57)	1.0×10^{-7}	1.95 (1.52–2.51)	1.7×10^{-17}
rs738491	22	42,685,444	*SAMM50*	A[a]/G	162/170/60 (0.63)	266/448/220 (0.52)	1.2×10^{-6}	1.54 (1.30–1.83)	66/87/19 (0.64)	247/506/258 (0.49)	1.0×10^{-6}	1.79 (1.41–2.27)	3.9×10^{-11}
rs2073082	22	42,691,340	*SAMM50*	A/G[a]	28/142/221 (0.75)	102/419/413 (0.67)	5.0×10^{-5}	1.48 (1.22–1.78)	11/66/95 (0.74)	140/457/412 (0.63)	1.0×10^{-4}	1.67 (1.29–2.17)	1.0×10^{-7}
rs3761472	22	42,699,455	*SAMM50*	T/C[a]	80/186/126 (0.56)	326/430/178 (0.42)	3.0×10^{-10}	1.74 (1.47–2.06)	33/86/53 (0.56)	328/515/168 (0.42)	1.5×10^{-6}	1.74 (1.38–2.19)	1.5×10^{-14}
rs2143571	22	42,723,019	*SAMM50*	A[a]/G	124/185/81 (0.56)	184/427/323 (0.43)	3.9×10^{-9}	1.68 (1.42–1.99)	53/86/33 (0.56)	171/518/323 (0.42)	2.9×10^{-6}	1.71 (1.36–2.15)	3.5×10^{-13}
rs6006473	22	42,724,408	*SAMM50, PARVB*	A[a]/G	163/170/59 (0.63)	274/446/214 (0.53)	3.6×10^{-6}	1.96 (1.65–2.32)	67/86/19 (0.64)	257/506/248 (0.50)	3.4×10^{-6}	1.74 (1.38–2.21)	3.2×10^{-10}
rs5764455	22	42,729,857	*PARVB*	T[a]/C	115/180/97 (0.52)	164/422/348 (0.40)	3.0×10^{-8}	1.63 (1.38–1.93)	47/90/35 (0.53)	155/495/362 (0.40)	1.5×10^{-6}	1.74 (1.38–2.19)	1.6×10^{-12}
rs6006611	22	42,732,031	*PARVB*	A/G[a]	51/167/174 (0.66)	187/471/276 (0.55)	2.4×10^{-7}	1.58 (1.33–1.88)	17/72/83 (0.69)	213/502/296 (0.54)	2.3×10^{-7}	1.90 (1.49–2.43)	1.8×10^{-12}

P values were calculated by Cochran–Armitage trend test. Odds ratios (ORs) were calculated for risk allele with 95 % confidence interval (CI). Combined *P* values were obtained using Fisher's combined probability test

[a] Risk allele

NAFLD-1, NAFLD-2 and control-2 subjects. We also genotyped rs738409 since this SNP was most extensively examined. After adjusting for age, gender, and BMI, nine SNPs were strongly associated with NAFLD ($P < 1.0 \times 10^{-9}$, Supplementary Table 1). SNP rs738409 was most strongly associated with NAFLD before adjustment ($P = 2.1 \times 10^{-18}$); however, after adjustment, eight SNPs (rs2896019, rs3810622, rs738491, rs3761472, rs2143571, rs6006473, rs5764455, and rs6006611) had also smaller P values (1.8×10^{-10} to 1.8×10^{-13}) compared to rs738409 ($P = 6.8 \times 10^{-14}$). Moreover, nine SNPs had high odds ratios (OR 1.84–2.05).

When eight SNPs were adjusted with rs738409 using NAFLD-1, NAFLD-2 and control-2 subjects, no SNPs showed significant association (Supplementary Table 2). P value of rs738409 was smaller than other SNPs, suggesting that rs738409 is most important for the development of NAFLD. We also examined association between 3-SNP (rs738409, rs2896019, and rs3810622) haplotype in the *PNPLA3*, 4-SNP (rs738491, rs3761472, rs2143571, and rs6006473) haplotype in the *SAMM50*, and 2 SNPs (rs5764455, and rs6006611) haplotype in the *PARVB* genes, and NAFLD, using NAFLD-1, NAFLD-2 and control-2 subjects. Haplotype GGA in the *PNPLA3* ($P = 1.3 \times 10^{-13}$, OR = 2.19), ACAA in the *SAMM50* ($P = 1.3 \times 10^{-11}$, OR = 1.99), and TG in the *PARVB* ($P = 5.0 \times 10^{-12}$, OR = 2.06) genes were strongly associated with NAFLD (Supplementary Table 3). Haplotype analysis suggested that *PNPLA3* gene is most important for the pathogenesis for NAFLD.

Analysis of various quantitative and histological phenotypes

Next, we investigated metabolic traits and NAFLD-susceptible SNPs since NAFLD is considered to be a part of metabolic syndrome (Marchesini et al. 2001; Stefan et al. 2008). Nine SNPs were associated with decreased serum triglycerides in NAFLD patients, but not in the control group (Table 3). Allelic effects on decreased triglycerides levels in NAFLD patients were similar among the nine SNPs. These SNPs were associated with increased AST and ALT both in NAFLD and control subjects. Allelic effects of SNPs in the *PNPLA3* gene on increased AST levels in NAFLD patients were higher than those of other SNPs. Other metabolic traits were not associated with the nine SNPs.

The nine SNPs were associated with lobular inflammation, ballooning, and NAS (Table 4). Rs3810622 was not associated with lobular inflammation. Six SNPs (rs738409, rs2896019, rs738491, rs6006473, rs5764455, and rs6006611) were associated with fibrosis. Allelic effects on NAS and fibrosis of SNPs in the *PNPLA3* and *PARVB* gene were stronger than those in the *SAMM50* genes, although the associations were not significant according to multiple testing. Nine SNPs in the chromosome 22q13 region were associated with increased serum ferritin (except rs5764455). Five SNPs in the *SAMMM50* and *PARVB* genes (rs738491, rs3761472, rs2143571, rs6006473, and 5764455) were associated with hyaluronic acid, which were high in NASH. No SNPs were associated with type IV collagen 7s. Nine SNPs showed different association levels with serum metabolic traits and histological severity suggesting that three genes (*PNPLA3*, *SAMM50*, and *PARVB*) may be involved in both the development and progression of NAFLD (Supplementary Fig. 4).

We have also performed the association tests of nine SNPs in patients with NASH and simple steatosis diagnosed by liver biopsy. Although the number of simple steatosis was small, nine SNPs were associated with NASH (OR = 1.76–2.79, Supplementary Table 4). Rs5764455 in the *PARVB* gene was most strongly associated with NASH ($P = 3.4 \times 10^{-6}$, OR = 2.79). Haplotype analysis revealed that most strongly association with steatosis was haplotype GGA in the *PNPLA3* ($P = 5.0 \times 10^{-4}$) and that haplotype TG in the *PARVB* gene was most strongly associated with NAS ($P = 9.6 \times 10^{-7}$) and fibrosis ($P = 4.4 \times 10^{-4}$, Supplementary Table 5).

Discussion

To elucidate the genetic background of NAFLD, we identified the candidate genes (Yoneda et al. 2008, 2009a, b; Hotta et al. 2010). We performed GWAS and found that the *PNPLA3-SAMM50-PARVB* genetic region was significantly associated with NAFLD in the Japanese population. According to our previous study (Hotta et al. 2010), rs738409 in the *PNPLA3* gene was most strongly associated with NAFLD. NAFLD patients are overweight to obese, and many have metabolic syndrome (Marchesini et al. 2001; Stefan et al. 2008). Even after adjusting for age, gender, and BMI, three SNPs (rs738409, rs2896019, and rs3810622) in the *PNPLA3*, four SNPs (rs738491, rs3761472, rs2143571, and rs6006473) in the *SAMM50*, and two SNPs (rs5764455 and rs6006611) in the *PARVB* genes showed significant P values. Our previous study indicated that the P value for the association between rs738409 and NAFLD increased after adjusting for age, gender, and BMI (Hotta et al. 2010). A recently reported GWAS showed the strongest association of rs738409 in the *PNPLA3* gene with NAFLD in the Japanese population; however, the study did not adjust for age, gender, or BMI (Kawaguchi et al. 2012). Although numerous reports and a meta-analysis have indicated that rs738409 is associated

Table 3 Association between significant SNPs and metabolic traits

SNP ID	Subjects	FPG (mg/dL)		T. Chol. (mg/dL)		Triglycerides (mg/dL)		HDL-C (mg/dL)	
		β (SE)	*P* value	β (SE)	*P* value	β (SE)	*P* value	β (SE)	*P* value
rs738409	Control-2	0.002 (0.003)	0.38	−0.269 (1.579)	0.86	0.007 (0.010)	0.47	0.518 (0.630)	0.41
	NAFLD-1,2	0.001 (0.006)	0.84	−2.732 (2.458)	0.27	−0.049 (0.013)	1.3×10^{-4}	0.463 (0.863)	0.59
rs2896019	Control-2	0.003 (0.003)	0.36	−0.862 (1.575)	0.58	0.011 (0.010)	0.26	0.390 (0.629)	0.54
	NAFLD-1,2	0.002 (0.006)	0.78	−2.750 (2.438)	0.26	−0.044 (0.013)	5.0×10^{-4}	0.448 (0.855)	0.60
rs3810622	Control-2	0.000 (0.003)	0.91	−0.260 (1.597)	0.87	0.011 (0.010)	0.25	0.396 (0.638)	0.53
	NAFLD-1,2	−0.003 (0.007)	0.69	−0.723 (2.621)	0.78	−0.047 (0.014)	5.1×10^{-4}	0.667 (0.915)	0.47
rs738491	Control-2	0.004 (0.003)	0.19	0.084 (1.555)	0.96	0.010 (0.009)	0.28	0.779 (0.620)	0.21
	NAFLD-1,2	0.005 (0.006)	0.40	−4.251 (2.558)	0.097	−0.041 (0.013)	0.0024	−0.023 (0.895)	0.98
rs3761472	Control-2	0.002 (0.003)	0.44	−0.277 (1.607)	0.86	0.008 (0.010)	0.39	0.618 (0.642)	0.34
	NAFLD-1,2	0.003 (0.006)	0.66	−3.636 (2.491)	0.15	−0.051 (0.013)	9.1×10^{-5}	0.394 (0.874)	0.65
rs2143571	Control-2	0.004 (0.003)	0.19	−0.017 (1.608)	0.99	0.010 (0.010)	0.30	0.548 (0.642)	0.39
	NAFLD-1,2	0.002 (0.006)	0.71	−3.789 (2.494)	0.13	−0.052 (0.013)	6.3×10^{-5}	0.325 (0.876)	0.71
rs6006473	Control-2	0.005 (0.003)	0.055	0.191 (1.554)	0.90	0.012 (0.009)	0.21	0.515 (0.620)	0.41
	NAFLD-1,2	0.005 (0.006)	0.42	−4.341 (2.559)	0.090	−0.042 (0.013)	0.0016	−0.123 (0.896)	0.89
rs5764455	Control-2	0.005 (0.003)	0.077	0.017 (1.610)	0.99	0.013 (0.010)	0.18	1.004 (0.642)	0.12
	NAFLD-1,2	0.002 (0.006)	0.74	−1.593 (2.453)	0.52	−0.042 (0.013)	0.0011	−0.097 (0.859)	0.91
rs6006611	Control-2	0.002 (0.003)	0.41	0.060 (1.561)	0.97	0.012 (0.009)	0.21	0.934 (0.623)	0.13
	NAFLD-1,2	0.000 (0.007)	0.97	−1.181 (2.608)	0.65	−0.039 (0.014)	0.0045	−0.627 (0.906)	0.49
SNP ID	Subjects	SBP (mmHg)		DBP (mmHg)		AST (IU/L)		ALT (IU/L)	
		β (SE)	*P* value	β (SE)	*P* value	β (SE)	*P* value	β (SE)	*P* value
rs738409	Control-2	0.271 (0.726)	0.71	−0.571 (0.462)	0.22	0.026 (0.007)	2.4×10^{-4}	0.032 (0.009)	4.4×10^{-4}
	NAFLD-1,2	0.383 (1.135)	0.74	−0.101 (0.904)	0.91	0.063 (0.013)	1.2×10^{-6}	0.073 (0.015)	1.1×10^{-6}
rs2896019	Control-2	0.422 (0.724)	0.56	−0.337 (0.462)	0.47	0.025 (0.007)	3.5×10^{-4}	0.032 (0.009)	4.3×10^{-4}
	NAFLD-1,2	0.275 (1.121)	0.81	0.016 (0.893)	0.99	0.063 (0.013)	1.2×10^{-6}	0.071 (0.015)	1.9×10^{-6}
rs3810622	Control-2	−0.134 (0.734)	0.85	−0.534 (0.468)	0.25	0.016 (0.007)	0.022	0.020 (0.009)	0.033
	NAFLD-1,2	0.719 (1.240)	0.56	0.991 (0.987)	0.32	0.053 (0.014)	1.3×10^{-4}	0.050 (0.016)	0.0018
rs738491	Control-2	0.441 (0.714)	0.54	−0.333 (0.455)	0.47	0.021 (0.007)	0.0024	0.027 (0.009)	0.0027
	NAFLD-1,2	−0.006 (1.172)	1.00	−0.111 (0.933)	0.91	0.049 (0.014)	2.9×10^{-4}	0.052 (0.016)	9.5×10^{-4}
rs3761472	Control-2	0.278 (0.739)	0.71	−0.430 (0.471)	0.36	0.022 (0.007)	0.0018	0.030 (0.009)	0.0011
	NAFLD-1,2	−0.223 (1.144)	0.85	−0.079 (0.911)	0.93	0.047 (0.013)	4.2×10^{-4}	0.054 (0.015)	4.2×10^{-4}
rs2143571	Control-2	0.258 (0.739)	0.73	−0.499 (0.471)	0.29	0.022 (0.007)	0.0022	0.030 (0.009)	0.0013
	NAFLD-1,2	−0.095 (1.137)	0.93	−0.133 (0.905)	0.88	0.047 (0.013)	3.6×10^{-4}	0.054 (0.015)	4.4×10^{-4}
rs6006473	Control-2	0.292 (0.714)	0.68	−0.391 (0.455)	0.39	0.020 (0.007)	0.0041	0.028 (0.009)	0.0024
	NAFLD-1,2	0.156 (1.167)	0.89	−0.195 (0.930)	0.83	0.049 (0.014)	3.5×10^{-4}	0.053 (0.016)	6.9×10^{-4}
rs5764455	Control-2	0.213 (0.740)	0.77	−0.500 (0.471)	0.29	0.015 (0.007)	0.034	0.025 (0.009)	0.0070
	NAFLD-1,2	−0.414 (1.122)	0.71	0.059 (0.894)	0.95	0.046 (0.013)	4.0×10^{-4}	0.050 (0.015)	9.7×10^{-4}
rs6006611	Control-2	0.151 (0.718)	0.83	−0.492 (0.457)	0.28	0.018 (0.007)	0.012	0.026 (0.009)	0.0046
	NAFLD-1,2	0.102 (1.217)	0.93	0.701 (0.969)	0.47	0.043 (0.014)	0.0018	0.050 (0.016)	0.0019

Data were derived from linear regression analysis. NAFLD-1, NAFLD-2 and control-2 were used for analysis. Values of FPG, triglycerides, AST, and ALT were logarithmically transformed. Each metabolic phenotype was adjusted for age, gender, and logarithmically transformed BMI

AST aspartate transaminase, *ALT* alanine transaminase, *DBP* diastolic blood pressure, *FPG* fasting plasma glucose, *HDL-C* high-density lipoprotein cholesterol, *SBP* systolic blood pressure, *SNP* single-nucleotide polymorphism, *T. Chol.* total cholesterol

with NAFLD (Sookoian and Pirola 2011) and that the *PNPLA3* gene is thought to be responsible for the NAFLD, we demonstrated that *SAMM50*, and *PARVB*, and *PNPLA3* are probably involved in NAFLD development.

NAFLD-susceptible SNPs were also associated with histological severity; however, the effects differed among the nine SNPs. Steatosis grade was equally affected by the nine SNPs. Association with histological activity (NAS)

Table 4 Association between SNPs and histological traits and serum biomarker in NAFLD-1 and NAFLD-2 subjects

SNP ID	Steatosis grade[a]		Lobular inflammation[a]		Hepatocyte ballooning[a]		NAS[a]	
	β (SE)	*P* value	β (SE)	*P* value	β (SE)	*P* value	β (SE)	*P* value
rs738409	0.136 (0.043)	0.0016	0.155 (0.044)	5.4×10^{-4}	0.137 (0.043)	0.0014	0.440 (0.097)	7.3×10^{-6}
rs2896019	0.141 (0.042)	9.7×10^{-4}	0.148 (0.044)	8.1×10^{-4}	0.137 (0.042)	0.0013	0.438 (0.096)	6.5×10^{-6}
rs3810622	0.147 (0.046)	0.0014	0.086 (0.048)	0.072	0.141 (0.046)	0.0023	0.395 (0.105)	1.9×10^{-4}
rs738491	0.116 (0.045)	0.0095	0.126 (0.046)	0.0069	0.131 (0.045)	0.0035	0.393 (0.102)	1.3×10^{-4}
rs3761472	0.131 (0.044)	0.0028	0.109 (0.045)	0.017	0.123 (0.044)	0.0052	0.387 (0.100)	1.2×10^{-4}
rs2143571	0.127 (0.044)	0.0039	0.106 (0.046)	0.021	0.120 (0.044)	0.0068	0.377 (0.100)	1.9×10^{-4}
rs6006473	0.103 (0.045)	0.022	0.118 (0.046)	0.011	0.134 (0.045)	0.0028	0.375 (0.102)	2.7×10^{-4}
rs5764455	0.113 (0.043)	0.0091	0.155 (0.044)	5.2×10^{-4}	0.136 (0.043)	0.0016	0.426 (0.098)	1.6×10^{-5}
rs6006611	0.122 (0.045)	0.0074	0.152 (0.047)	0.0012	0.189 (0.045)	2.7×10^{-5}	0.475 (0.102)	4.1×10^{-6}
SNP ID	Fibrosis[a]		Ferritin (ng/ml)		Hyaluronic acid (ng/dL)		Type IV collagen 7s (ng/dL)	
	β (SE)	*P* value	β (SE)	*P* value	β (SE)	*P* value	β (SE)	*P* value
rs738409	0.180 (0.062)	0.0036	0.076 (0.025)	0.0028	0.042 (0.023)	0.061	0.003 (0.010)	0.77
rs2896019	0.183 (0.061)	0.0029	0.072 (0.025)	0.0044	0.042 (0.022)	0.062	0.004 (0.010)	0.66
rs3810622	0.110 (0.066)	0.097	0.083 (0.027)	0.0023	0.045 (0.024)	0.064	0.010 (0.011)	0.36
rs738491	0.149 (0.064)	0.021	0.066 (0.026)	0.013	0.079 (0.023)	7.8×10^{-4}	0.006 (0.011)	0.60
rs3761472	0.091 (0.063)	0.15	0.087 (0.026)	8.7×10^{-4}	0.069 (0.023)	0.0028	0.009 (0.010)	0.37
rs2143571	0.101 (0.063)	0.11	0.089 (0.026)	6.5×10^{-4}	0.066 (0.023)	0.0039	0.009 (0.011)	0.37
rs6006473	0.157 (0.064)	0.015	0.071 (0.026)	0.0076	0.072 (0.023)	0.0022	0.005 (0.011)	0.65
rs5764455	0.222 (0.061)	3.3×10^{-4}	0.046 (0.025)	0.068	0.059 (0.022)	0.0083	0.001 (0.010)	0.95
rs6006611	0.195 (0.065)	0.0027	0.057 (0.027)	0.033	0.041 (0.024)	0.089	0.004 (0.011)	0.73

Data were derived from linear regression analysis. NAFLD-1, NAFLD-2 and control-2 were used for analysis. Values of ferritin, hyaluronic acid, and type IV collagen 7s were logarithmically transformed. Each phenotype was adjusted for age, gender, and logarithmically transformed BMI

[a] Histological diagnosed patients from NAFLD-1 ($n = 392$) and NAFLD-2 ($n = 101$) subjects were used for analysis

and severity (fibrosis stage) of NAFLD were stronger with SNPs in the *PNPLA3* and *PARVB* genes. Among biomarkers, AST and ALT, which are commonly used to evaluate liver function, were highly associated with the two SNPs in the *PNPLA3* gene, in NAFLD and in the control subjects. Ferritin and hyaluronic acid, the level of which increase in NASH, were associated with SNPs in the *SAMM50* gene. SNP in the *PARVB* gene also showed strong association with NASH compared with simple steatosis. Haplotype analysis indicated that *PNPLA3* gene would be most important for the development for NAFLD and that *PARVB* gene would be most important for the progression of NAFLD. Our data suggested that SNPs in *PNPLA3*, *SAMM50* and *PARVB* contribute to the increased NAFLD activity, resulting in the progression from simple steatosis to NASH. It has been suggested that NASH is induced in two consecutive steps (the so-called 2-hit hypothesis): (i) excess fat accumulation in the liver and (ii) subsequent necroinflammation in the liver (Day and James 1998). Our results indicate that SNPs in *PNPLA3* may be involved in the first hit and that SNPs in *PNPLA3*, *SAMM50* and *PARVB* may be involved in the second hit. The associations were not significant for multiple tests; therefore, further analysis is necessary.

We previously reported that rs738409 is associated with decreased serum triglycerides in NAFLD patients (Hotta et al. 2010). In this study, we observed that SNPs, particularly in the *SAMM50* gene, were associated with deceased levels of serum triglycerides. The association between SNPs in the *PNPLA3* gene and decreased triglycerides levels in NAFLD is controversial (Kollerits et al. 2009; Speliotes et al. 2010, 2011). Recent reports indicate that rs738409 are associated with decreased serum triglycerides in type 2 diabetes (Palmer et al. 2012; Krarup et al. 2012). The controversy may be due in part to the observation that SNPs in the *SAMM50* gene showed a stronger effect on triglyceride levels than the SNP in the *PNPLA3* gene. Further investigation is necessary to elucidate the association between SNPs in *PNPLA3* and *SAMM50* genes and serum triglycerides levels.

PNPLA3 rs738409 has been extensively investigated, and a strong association with NAFLD has been confirmed

(Day and James 1998). The *PNPLA3* gene is thought to be involved in abnormal lipid metabolism in the liver of NAFLD patients. *PNPLA3*-deficient mice and transgenic mice did not show a fatty liver (Chen et al. 2010; Basantani et al. 2011; Li et al. 2012). Overexpression of $PNPLA3^{I148M}$ in mouse liver developed to fatty liver, but not into NASH (Li et al. 2012). Thus, PNPLA3 plays an important in the development, but not in the progression of NAFLD. Our study suggests that the *SAMM50* and *PARVB* genes may also be involved in the progression (necroinflammation and fibrosis) of NAFLD. Sam50, encoded by the *SAMM50* gene, is a member of the sorting and assembly machinery for β-barrel proteins in the mitochondrial outer membrane. Sam50 was reported to be involved in the structural integrity of mitochondrial cristae, assembly of respiratory complexes, and maintenance of mitochondrial DNA. Long-term depletion of Sam50 influences the amounts of proteins in all the large respiratory complexes in the mitochondria (Ott et al. 2012). Mitochondrial abnormalities (loss of mitochondrial cristae and paracrystalline inclusions) have been described for liver biopsy specimens of patients with NASH (Sanyal et al. 2001; Caldwell et al. 1999). These reports and our results suggest that the *SAMM50* gene may be involved in mitochondrial dysfunction and subsequent decreased removal of reactive oxygen species (ROS), leading to progression of NAFLD. The *PARVB* gene encodes parvin-β, which forms integrin-linked kinase-pinch-parvin complex, transmits signals from integrin to Akt/protein kinase B (PKB) (Kimura et al. 2010). Integrins are a large family of heterodimeric cell surface receptors that act as mechanoreceptors by relaying information between cells and from the extracellular matrix (ECM) to the cell interior. Since integrin receptors directly bind to ECM components to control remodeling, they are thought to play a crucial role in the evolution and progression of liver fibrosis (Desgrosellier and Cheresh 2010; Patsenker and Stickel 2011). Loss of parvin-β contributes to increased integrin-linked kinase activity and cell–matrix adhesion. Overexpression of parvin-β increases mRNA expression, serine 82 phosphorylation, and activity of peroxisome proliferator-activated receptor γ (PPARγ), leading to a concomitant increase in lipogenic gene expression (Johnstone et al. 2008). Our data and previous reports suggest that the *PARVB* gene is involved in lipid accumulation and/or fibrosis in the liver, resulting in NAFLD.

In summary, we demonstrated that polymorphisms in the *SAMM50* and *PARVB* genes, as well as those in the*PNPLA3* gene, were associated with NAFLD development and progression. SNPs in the *PNPLA3* gene may be involved in the first hit and the *SAMM50* and *PARVB* genes (and *PNPLA3* gene) in the second hit, although further studies are necessary to confirm our results.

Acknowledgments This work was supported by a Grant-in-Aid from the Ministry of Education, Science, Sports, and Culture of Japan (21591186 to K. H, 23791027 to A. K., and 23701082 to T. K.).

Conflict of interest The authors declare that they have no conflict of interest.

References

Angulo P (2002) Nonalcoholic fatty liver disease. N Engl J Med 18:1221–1231

Barrett JC, Fry B, Maller J, Daly MJ (2005) Haploview: analysis and visualization of LD and haplotype maps. Bioinformatics 21:263–265

Basantani MK, Sitnick MT, Cai L, Brenner DS, Gardner NP, Li JZ, Schoiswohl G, Yang K, Kumari M, Gross RW, Zechner R, Kershaw EE (2011) Pnpla3/adiponutrin deficiency in mice does not contribute to fatty liver disease or metabolic syndrome. J Lipid Res 52:318–329

Brunt EM (2001) Nonalcoholic steatohepatitis: definition and pathology. Semin Liver Dis 21:3–16

Caldwell SH, Swerdlow RH, Khan EM, Iezzoni JC, Hespenheide EE, Parks JK, Parker WD Jr (1999) Mitochondrial abnormalities in non-alcoholic steatohepatitis. J Hepato l 31:430–434

Chalasani N, Guo X, Loomba R, Goodarzi MO, Haritunians T, Kwon S, Cui J, Taylor KD, Wilson L, Cummings OW, Chen YD, Rotter JI, Nonalcoholic Steatohepatitis Clinical Research Network (2010) Genome-wide association study identifies variants associated with histologic features of nonalcoholic Fatty liver disease. Gastroenterology 139:1567–1576

Chen W, Chang B, Li L, Chan L (2010) Patatin-like phospholipase domain-containing 3/adiponutrin deficiency in mice is not associated with fatty liver disease. Hepatology 52:1134–1142

Day CP, James OF (1998) Steatohepatitis: a tale of two "hits"? Gastroenterology 114:842–845

Desgrosellier JS, Cheresh DA (2010) Integrins in cancer: biological implications and therapeutic opportunities. Nat Rev Cancer 10:9–22

Farrell GC (2003) Non-alcoholic steatohepatitis: what is it, and why is it important in the Asia-Pacific region? J Gastroenterol Hepatol 18:124–138

Hotta K, Yoneda M, Hyogo H, Ochi H, Mizusawa S, Ueno T, Chayama K, Nakajima A, Nakao K, Sekine A (2010) Association of the rs738409 polymorphism in PNPLA3 with liver damage and the development of nonalcoholic fatty liver disease. BMC Med Genet 11:172

Johnstone CN, Mongroo PS, Rich AS, Schupp M, Bowser MJ, Delemos AS, Tobias JW, Liu Y, Hannigan GE, Rustgi AK (2008) Parvin-beta inhibits breast cancer tumorigenicity and promotes CDK9-mediated peroxisome proliferator-activated receptor gamma 1 phosphorylation. Mol Cell Biol 28:687–704

Kawaguchi T, Sumida Y, Umemura A, Matsuo K, Takahashi M, Takamura T, Yasui K, Saibara T, Hashimoto E, Kawanaka M, Watanabe S, Kawata S, Imai Y, Kokubo M, Shima T, Park H, Tanaka H, Tajima K, Yamada R, Matsuda F, Takeshi O, Japan Study Group of Nonalcoholic Fatty Liver Disease (2012) Genetic polymorphisms of the human PNPLA3 gene are strongly associated with severity of non-alcoholic fatty liver disease in Japanese. PLoS One 7:e38322

Kimura M, Murakami T, Kizaka-Kondoh S, Itoh M, Yamamoto K, Hojo Y, Takano M, Kario K, Shimada K, Kobayashi E (2010) Functional molecular imaging of ILK-mediated Akt/PKB

signaling cascades and the associated role of beta-parvin. J Cell Sci 123:747–755

Kleiner DE, Brunt EM, Van Natta M, Behling C, Contos MJ, Cummings OW, Ferrell LD, Liu YC, Torbenson MS, Unalp-Arida A, Yeh M, McCullough AJ, Sanyal AJ, Nonalcoholic Steatohepatitis Clinical Research Network (2005) Design and validation of a histological scoring system for nonalcoholic fatty liver disease. Hepatology 41:1313–1321

Kollerits B, Coassin S, Beckmann ND, Teumer A, Kiechl S, Döring A, Kavousi M, Hunt SC, Lamina C, Paulweber B, Kutalik Z, Nauck M, van Duijn CM, Heid IM, Willeit J, Brandstätter A, Adams TD, Mooser V, Aulchenko YS, Völzke H, Kronenberg F (2009) Genetic evidence for a role of adiponutrin in the metabolism of apolipoprotein B-containing lipoproteins. Hum Mol Genet 18:4669–4676

Krarup NT, Grarup N, Banasik K, Friedrichsen M, Færch K, Sandholt CH, Jørgensen T, Poulsen P, Witte DR, Vaag A, Sørensen T, Pedersen O, Hansen T (2012) The PNPLA3 rs738409 G-allele associates with reduced fasting serum triglyceride and serum cholesterol in Danes with impaired glucose regulation. PLoS ONE 7:e40376

Li JZ, Huang Y, Karaman R, Ivanova PT, Brown HA, Roddy T, Castro-Perez J, Cohen JC, Hobbs HH (2012) Chronic overexpression of PNPLA3I148 M in mouse liver causes hepatic steatosis. J Clin Invest, in press. doi:10.1172/JCI65179

Ludwig J, Viggiano TR, McGill DB, Oh BJ (1980) Nonalcoholic steatohepatitis: Mayo clinic experiences with a hitherto unnamed disease. Mayo Clin Proc 55:434–438

Marchesini G, Brizi M, Bianchi G, Tomassetti S, Bugianesi E, Lenzi M, McCullough AJ, Natale S, Forlani G, Melchionda N (2001) Nonalcoholic fatty liver disease: a feature of the metabolic syndrome. Diabetes 50:1844–1850

Matteoni CA, Younossi ZM, Gramlich T, Boparai N, Liu YC, McCullough AJ (1999) Nonalcoholic fatty liver disease: a spectrum of clinical and pathological severity. Gastroenterology 116:1413–1419

Nielsen DM, Ehm MG, Weir BS (1998) Detecting marker-disease association by testing for Hardy–Weinberg disequilibrium at a marker locus. Am J Hum Genet 63:1531–1540

Ohnishi Y, Tanaka T, Ozaki K, Yamada R, Suzuki H, Nakamura Y (2001) A high-throughput SNP typing system for genome-wide association studies. J Hum Genet 46:471–477

Ott C, Ross K, Straub S, Thiede B, Götz M, Goosmann C, Krischke M, Mueller MJ, Krohne G, Rudel T, Kozjak-Pavlovic V (2012) Sam50 functions in mitochondrial intermembrane space bridging and biogenesis of respiratory complexes. Mol Cell Biol 32:1173–1188

Palmer CN, Maglio C, Pirazzi C, Burza MA, Adiels M, Burch L, Donnelly LA, Colhoun H, Doney AS, Dillon JF, Pearson ER, McCarthy M, Hattersley AT, Frayling T, Morris AD, Peltonen M, Svensson PA, Jacobson P, Borén J, Sjöström L, Carlsson LM, Romeo S (2012) Paradoxical lower serum triglyceride levels and higher type 2 diabetes mellitus susceptibility in obese individuals with the PNPLA3 148 M variant. PLoS ONE 7:e39362

Patsenker E, Stickel F (2011) Role of integrins in fibrosing liver diseases. Am J Physiol Gastrointest Liver Physiol 301:G425–G434

Purcell S, Neale B, Todd-Brown K, Thomas L, Ferreira MA, Bender D, Maller J, Sklar P, de Bakker PI, Daly MJ, Sham PC (2007) PLINK: a tool set for whole-genome association and population-based linkage analyses. Am J Hum Genet 81:559–575

Romeo S, Kozlitina J, Xing C, Pertsemlidis A, Cox D, Pennacchio LA, Boerwinkle E, Cohen JC, Hobbs HH (2008) Genetic variation in PNPLA3 confers susceptibility to nonalcoholic fatty liver disease. Nat Genet 40:1461–1465

Sanyal AJ (2002) American Gastroenterological Association: AGA technical review on nonalcoholic fatty liver disease. Gastroenterology 123:1705–1725

Sanyal AJ, Campbell-Sargent C, Mirshahi F, Rizzo WB, Contos MJ, Sterling RK, Luketic VA, Shiffman ML, Clore JN (2001) Nonalcoholic steatohepatitis: association of insulin resistance and mitochondrial abnormalities. Gastroenterology 120:1183–1192

Sookoian S, Pirola CJ (2011) Meta-analysis of the influence of I148 M variant of patatin-like phospholipase domain containing 3 gene (PNPLA3) on the susceptibility and histological severity of nonalcoholic fatty liver disease. Hepatology 53:1883–1894

Speliotes EK, Butler JL, Palmer CD, Voight BF, GIANT Consortium; MIGen Consortium; NASH CRN, Hirschhorn JN (2010) PNPLA3 variants specifically confer increased risk for histologic nonalcoholic fatty liver disease but not metabolic disease. Hepatology 52:904–912

Speliotes EK, Yerges-Armstrong LM, Wu J, Hernaez R, Kim LJ, Palmer CD, Gudnason V, Eiriksdottir G, Garcia ME, Launer LJ, Nalls MA, Clark JM, Mitchell BD, Shuldiner AR, Butler JL, Tomas M, Hoffmann U, Hwang SJ, Massaro JM, O'Donnell CJ, Sahani DV, Salomaa V, Schadt EE, Schwartz SM, Siscovick DS; NASH CRN; GIANT Consortium; MAGIC Investigators, Voight BF, Carr JJ, Feitosa MF, Harris TB, Fox CS, Smith AV, Kao WH, Hirschhorn JN, Borecki IB; GOLD Consortium (2011) Genome-wide association analysis identifies variants associated with nonalcoholic fatty liver disease that have distinct effects on metabolic traits. PLoS Genet 7:e1001324

Stefan N, Kantartzis K, Häring HU (2008) Causes and metabolic consequences of fatty liver. Endocr Rev 29:939–960

Teli MR, James OF, Burt AD, Bennett MK, Day CP (1995) The natural history of nonalcoholic fatty liver: a follow-up study. Hepatology 22:1714–1719

Wilfred de Alwis NM, Day CP (2008) Genes and nonalcoholic fatty liver disease. Curr Diab Rep 8:156–163

Yoneda M, Hotta K, Nozaki Y, Endo H, Uchiyama T, Mawatari H, Iida H, Kato S, Hosono K, Fujita K, Yoneda K, Takahashi H, Kirikoshi H, Kobayashi N, Inamori M, Abe Y, Kubota K, Saito S, Maeyama S, Wada K, Nakajima A (2008) Association between PPARGC1A polymorphisms and the occurrence of nonalcoholic fatty liver disease (NAFLD). BMC Gastroenterol 8:27–34

Yoneda M, Hotta K, Nozaki Y, Endo H, Uchiyama T, Mawatari H, Iida H, Kato S, Fujita K, Takahashi H, Kirikoshi H, Kobayashi N, Inamori M, Abe Y, Kubota K, Saito S, Maeyama S, Wada K, Nakajima A (2009a) Association between angiotensin II type 1 receptor polymorphisms and the occurrence of nonalcoholic fatty liver disease. Liver Int 29:1078–1085

Yoneda M, Hotta K, Nozaki Y, Endo H, Tomeno W, Watanabe S, Hosono K, Mawatari H, Iida H, Fujita K, Takahashi H, Kirikoshi H, Kobayashi N, Inamori M, Kubota K, Shimamura T, Saito S, Maeyama S, Wada K, Nakajima A (2009b) Influence of inducible nitric oxide synthase polymorphisms in Japanese patients with non-alcoholic fatty liver disease. Hepatol Res 39:963–971

Endocrine Journal 2013, **60** (4), 397-402

REVIEW

Vascular research using human pluripotent stem cells and humoral factors

Masakatsu Sone and Kazuwa Nakao

Department of Medicine and Clinical Science, Kyoto University Graduate School of Medicine, Kyoto 606-8507, Japan

Abstract. Embryonic stem (ES) cells are pluripotent cells collected from the inner cell mass of blastocysts. Induced pluripotent stem cells exhibit characteristics and pluripotency similar to ES cells, even though they were generated from adult somatic cells. We have been investigating the vascular differentiation kinetics of human pluripotent stem cells (PSCs) and their application to human vascular research and clinical medicine. In this review, we present an overview of recent vascular research using human PSCs, focusing on the role of humoral factors and their receptors. We also discuss possible future application of human PSCs to translational research on human vascular disorders.

Key words: Human induced pluripotent stem cell, Human embryonic stem cell, Vascular endothelial cell, Vascular smooth muscle cell, Vascular hormone

EMBRYONIC STEM (ES) cells are pluripotent cells collected from the inner cell mass of blastocysts. Mouse ES cells were first established by Evans *et al.* in 1981 [1]. Subsequent establishment of human ES cells was difficult owing to the many differences between mouse and primate ES cells [2]. After 17 years have passed since the establishment of mouse ES cells, human ES cells were first established by Thomon JA, *et al.* in 1998 [3]. Recently, induced pluripotent stem (iPS) cells were generated from both mouse and human somatic cells through the introduction of defined factors [4, 5, 6]. Although iPS cells are derived from adult somatic cells, their characteristics and pluripotency are nearly identical to those of ES cells. In this review, we present an overview of ongoing vascular research making use of pluripotent stem cells (PSCs), especially human PSCs, focusing on the roles of humoral factors and their receptors.

Induction of vascular cells from human PSCs

The differentiation of hemangioblast-like cells from mouse ES cells was first reported in 1998 [7]. Flk1-positive cells derived from mouse ES cells differentiated into sheet-like clusters of VE-cadherin- (CD144), PECAM-1- (CD31) and CD34-positive vascular endothelial cells when co-cultured with OP9 feeder cells [8]. Mural cells (i.e., vascular smooth muscle cells and pericytes) were also differentiated from the same Flk1-positive cells induced from mouse ES cells [9]. In primates, however, Flk1 is expressed even in undifferentiated ES cells, and the vascular differentiation kinetics differ from those of mouse ES cells [10]. In 2003, human ES cells were established in Japan, where we succeeded in inducing and isolating vascular endothelial cells and mural cells from human ES cells [11]. In the meanwhile, Yamanaka *et al.* established iPS cells from mouse and human fibroblasts [4, 5]. These iPS cells were capable of differentiating into vascular cells in the same manner as mouse and human ES cells [12, 13, 14]. Moreover, a modified serum and feeder-free method for the induction of vascular endothelial cells from human ES/iPS cells was recently reported [15, 16], and we are continuing to modify and refine the method for stable differentiation of various human iPS lines.

Vascular differentiation and humoral factors

Humoral factors and their receptors play key roles in the pathway along which human PSCs differentiate into vascular cells (Fig. 1). Flk1 (also known as

Submitted Jan. 16, 2013; Accepted Jan. 17, 2013 as EJ13-0020
Released online in J-STAGE as advance publication Jan. 31, 2013

Correspondence to: Masakatsu Sone, M.D., Ph.D., Department of Medicine and Clinical Science, Kyoto University Graduate School of Medicine, 54 Shogoin Kawahara-cho, Sakyo-ku, Kyoto 606-8507, Japan. E-mail: sonemasa@kuhp.kyoto-u.ac.jp

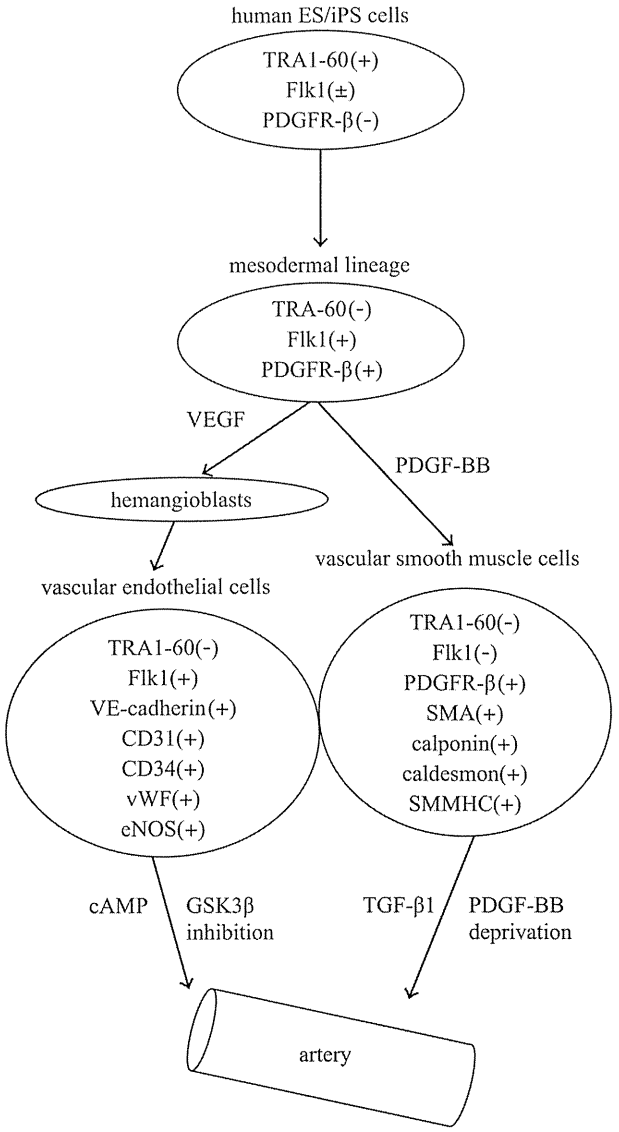

Fig. 1 Schematic representation of the role of humoral factors in the pathway of vascular differentiation from human PSCs TRA1, tumor rejection antigen 1; PDGF, platelet-derived growth factor; VEGF, vascular endothelial growth factor; Flk1, fetal liver kinase 1 (VEGF receptor 2); VE-cadherin, vascular endothelial cadherin; vWF, von Willebrand factor; eNOS, endothelial NO synthase; SMA, smooth muscle actin; SMMHC, smooth muscle myosin heavy chain

VEGFR-2) is one of the VEGF receptors and is known to be a marker of proximal lateral mesoderm in mouse [6]. Induction of vascular endothelial cells, mural cells and cardiomyocytes from Flk1-positive cells has been confirmed in both mouse and human ES cells [9, 11, 17, 18]. VEGF dose-dependently induces differentiation of Flk1-positive cells into vascular endothelial cells. In mouse ES cells, another VEGF receptor, Flt1 (also known as VEGFR-1), is expressed at a later phase of vascular differentiation, and the delayed expression of VEGFR-1 correlates with an increase in dose sensitivity to VEGF [19]. This VEGF dose sensitivity is also observed in human ES cells. These vascular differentiation processes of ES cells are almost identical in iPS cells [12, 14]. In mouse ES cells, adrenomedullin acts *via* its second messenger, cAMP, to induce arterial differentiation of vascular endothelial cells [20]. Notch and GSK3β-mediated β-catenin signaling is activated downstream of cAMP *via* phosphatidylinositol-3 kinase and induces differentiation to arterial endothelial cells [21]. Inhibition of GSK3β also induces arterial differentiation in human ES/iPS cells [16].

Vascular smooth muscle cells are believed to derive from mesoderm, neural crest or epicardial cells and to then migrate to form the vessel wall; however, difficulty in preparing pure populations of these lineages has hampered dissection of the mechanisms underlying vessel formation. It is reported that Flk1-positive cells derived from mouse ES cells can differentiate into both endothelial and vascular smooth muscle cells, and so they referred to these cells "vascular progenitor cells" [9]. In humans, some TRA1-60-negative cells derived from human ES cells express Flk1 and PDGF receptor β. Stimulation of these cells with VEGF induces vascular endothelial cells, while stimulation with PDGF-BB induces vascular smooth muscle-like cells [11]. In another recent study, human PSCs were induced to differentiate into the synthetic vascular smooth muscle cell phenotype in medium containing high serum with PDGF-BB and TGF-β1, after which serum starvation and PDGF-BB deprivation caused maturation towards the contractile vascular smooth muscle cell phenotype [22]. On the other hand, heterogeneity of embryological origins is a hallmark of vascular smooth muscle cells *in vivo*. In one study, for example, human PSCs were initially induced to form neuroectoderm, lateral plate mesoderm or paraxial mesoderm, and each of these intermediate populations was then further differentiated towards vascular smooth muscle cells. Notably, the derived vascular smooth muscle cell subtypes recapitulated the unique proliferative and secretory responses to cytokines previously documented in studies using aortic SMCs of distinct origins [23]. This result suggests heterogeneous origins in the development of vascular smooth muscle cells.

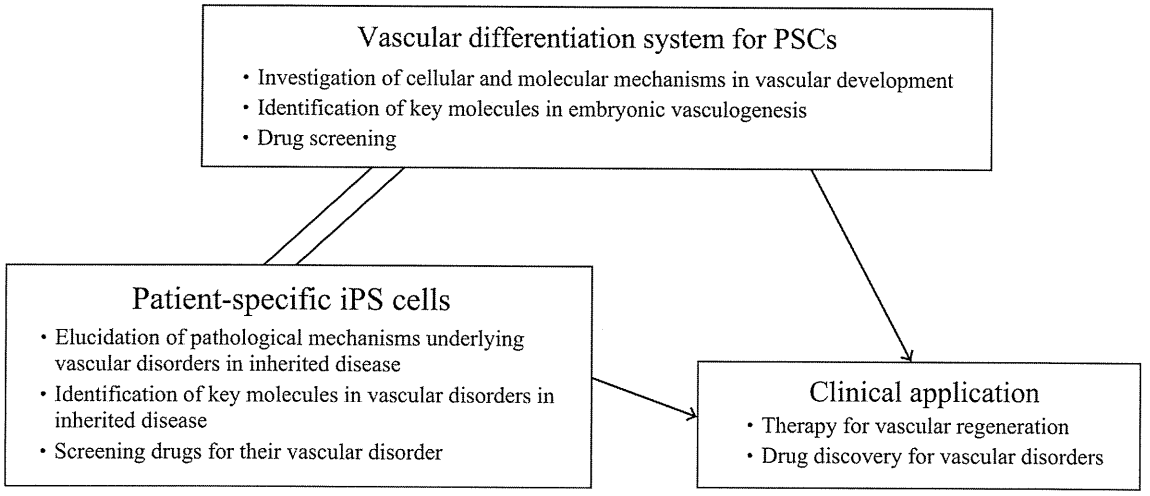

Fig. 2 Future applications of human iPS cells for vascular research

Future application of human iPS cells for vascular research

Vascular differentiation from PSCs is a productive area of basic research; however, clinical application of PSCs has not yet been achieved. Applications of a PSC-based vascular differentiation system can be separated to three categories (Fig. 2). The first is application for vascular regeneration therapy. As for somatic progenitor cells, after reports that bone marrow-derived CD34-positive mononuclear blood cells have the potential to differentiate into vascular endothelial cells and were referred to as "endothelial progenitor cells" (EPCs) [24], several clinical studies entailing transplantation of bone marrow stem cells as vascular regeneration therapy for ischemic diseases were performed [25-28]. In those studies, transplantation of bone marrow stem cells induced angiogenesis and relief of ischemic symptoms. Notably, however, the transplanted cells rarely survived as vascular endothelial cells, and the same effect was observed after transplantation of peripheral mononuclear blood cells [29]. Consequently, the clinical effect is not thought to be due to vessel formation by the transplanted cells, but to production of angiogenic factors. A report also showed that the implanted cells do not secrete angiogenic factors at levels sufficient to induce neovascularization; they instead stimulate muscle cells to produce angiogenic factors, thereby promoting neovascularization of ischemic tissues [30]. Vascular cells derived from human PSCs have been transplanted into animal models of ischemia in several studies [31-35], but no studies have yet been carried out in humans due to both ethical considerations and technical problems. So far, for example, transplanted vascular cells form only capillaries. Perhaps combining these cells with tissue engineering might lead to a breakthrough in their application [36-38].

The second application category is research into cell biology and drug discovery. Human PSC-based vascular differentiation systems enable one to observe and investigate the cellular and molecular mechanisms underlying vascular development *in vitro*. In addition, with these cells one can investigate the characteristics of vascular cells at early stages during differentiation. For example, we reported that Sirt1 expression is higher early during differentiation of vascular endothelial cells from human PSCs than it is in human adult endothelial cells, and that Sirt1 plays a key role in endothelial cell functions [16]. These systems might also enable identification of novel molecules responsible for embryonic vasculogenesis and support the discovery of new drugs for vascular regeneration therapy.

The third application category is research into the use of patient-specific iPS cells. iPS cells can be established from any human being, irrespective of their genetic background. The establishment of iPS cell lines from patients with inherited diseases presenting vascular abnormality should enable clarification of their pathogenesis. Patient-specific iPS cells are also useful for constructing *in vitro* models that can facilitate understanding of disease mechanisms and screening for more effective and safer drugs. For research

using patient-specific iPS cells, refined methods of differentiating and isolating cells for target tissue is indispensable. Although recently there has been a great deal of research into patient-specific iPS cells [39-52], research into their use in the vasculature and endocrine organs is still rare [53]. We are now investigating the pathogenesis of several inherited vascular disorders with collaborators.

Acknowledgement

We thank our laboratory members and collaborators for their helpful support and thoughtful discussion. Work carried out in our laboratories is supported by Grants-in-Aid for Scientific Research from the Japan Society for the Promotion of Science and grants from the Japanese Ministry of Health, Labour and Welfare.

References

1. Evans MJ, Kaufman MH (1981) Establishment in culture of pluripotential cells from mouse embryos. *Nature* 292(5819): 154-156.
2. Reubinoff BE, Pera MF, Fong CY, Trounson A, Bongso A (2000) Embryonic stem cell lines from human blastocysts: somatic differentiation in vitro. *Nat Biotechnol* 18: 399-404.
3. Thomson JA, Itskovitz-Eldor J, Shapiro SS, Waknitz MA, Jones JM, et al. (1998) Embryonic stem cell lines derived from human blastocysts. *Science* 282(5391): 1145-1147.
4. Takahashi K, Yamanaka S (2006) Induction of pluripotent stem cells from mouse embryonic and adult fibroblast cultures by defined factors. *Cell* 126(4): 663-676.
5. Takahashi K, Tanabe K, Ohnuki M, Narita M, Yamanaka S, et al. (2007) Induction of pluripotent stem cells from adult human fibroblasts by defined factors. *Cell* 131(5): 861-872.
6. Yu J, Vodyanik MA, Smuga-Otto K, Antosiewicz-Bourget J, Thomson JA, et al. (2007) Induced pluripotent stem cell lines derived from human somatic cells. *Science* 318(5858): 1917-1920.
7. Nishikawa SI, Nishikawa S, Hirashima M, Matsuyoshi N, Kodama H (1998) Progressive lineage analysis by cell sorting and culture identifies FLK1+VE-cadherin+ cells at a diverging point of endothelial and hemopoietic lineages. *Development* 125(9): 1747-1757.
8. Hirashima M, Kataoka H, Nishikawa S, Matsuyoshi N, Nishikawa S (1999) Maturation of embryonic stem cells into endothelial cells in an in vitro model of vasculogenesis. *Blood* 93(4): 1253-1263.
9. Yamashita J, Itoh H, Hirashima M, Ogawa M, Nishikawa S, et al. (2000) Flk1-positive cells derived from embryonic stem cells serve as vascular progenitors. *Nature* 408(6808): 92-96.
10. Sone M, Itoh H, Yamashita J, Yurugi-Kobayashi T, Nakao K, et al. (2003) Different differentiation kinetics of vascular progenitor cells in primate and mouse embryonic stem cells. *Circulation* 107(16): 2085-2088.
11. Sone M, Itoh H, Yamahara K, Yamashita JK, Nakao K, et al. (2007) Pathway for differentiation of human embryonic stem cells to vascular cell components and their potential for vascular regeneration. *Arterioscler Thromb Vasc Biol* 27(10): 2127-2134.
12. Narazaki G, Uosaki H, Teranishi M, Okita K, Yamashita JK, et al. (2008) Directed and systematic differentiation of cardiovascular cells from mouse induced pluripotent stem cells. *Circulation* 118(5): 498-506.
13. Choi KD, Yu J, Smuga-Otto K, Salvagiotto G, Slukvin I, et al. (2009) Hematopoietic and endothelial differentiation of human induced pluripotent stem cells. *Stem Cells* 27(3): 559-567.
14. Taura D, Sone M, Homma K, Oyamada N, Nakao K, et al. (2009) Induction and isolation of vascular cells from human induced pluripotent stem cells. *Arterioscler Thromb Vasc Biol* 29(7): 1100-1103.
15. Tatsumi R, Suzuki Y, Sumi T, Sone M, Nakatsuji N, et al. (2011) Simple and highly efficient method for production of endothelial cells from human embryonic stem cells. *Cell Transplant* 20(9): 1423-1430.
16. Homma K, Sone M, Taura D, Yamahara K, Nakao K, et al. (2010) Sirt1 plays an important role in mediating greater functionality of human ES/iPS-derived vascular endothelial cells. *Atherosclerosis* 212(1): 42-47.
17. Yamashita JK, Takano M, Hiraoka-Kanie M, Shimazu C, Nishikawa S, et al. (2005) Prospective identification of cardiac progenitors by a novel single cell-based cardiomyocyte induction. *FASEB J* 19(11): 1534-1536.
18. Yang L, Soonpaa MH, Adler ED, Roepke TK, Keller GM, et al. (2008) Human cardiovascular progenitor cells develop from a KDR+ embryonic-stem-cell-derived population. *Nature* 453(7194): 524-528.
19. Hirashima M, Ogawa M, Nishikawa S, Matsumura K, Nishikawa S, et al. (2003) A chemically defined culture of VEGFR2+ cells derived from embryonic stem cells reveals the role of VEGFR1 in tuning the threshold for VEGF in developing endothelial cells. *Blood* 101(6): 2261-2267.
20. Yurugi-Kobayashi T, Itoh H, Schroeder T, Nakano A, Yamashita JK, et al. (2006) Adrenomedullin/cyclic AMP pathway induces Notch activation and differentiation of arterial endothelial cells from vascular progeni-

tors. *Arterioscler Thromb Vasc Biol* 26(9): 1977-1984.
21. Yamamizu K, Matsunaga T, Uosaki H, Fukushima H, Yamashita JK, et al. (2010) Convergence of Notch and beta-catenin signaling induces arterial fate in vascular progenitors. *J Cell Biol* 189(2): 325-338.
22. Wanjare M, Kuo F, Gerecht S (2013) Derivation and maturation of synthetic and contractile vascular smooth muscle cells from human pluripotent stem cells. *Cardiovasc Res* 97: 321-330.
23. Cheung C, Bernardo AS, Trotter MW, Pedersen RA, Sinha S (2013) Generation of human vascular smooth muscle subtypes provides insight into embryological origin-dependent disease susceptibility. *Nat Biotechnol* 30(2): 165-173.
24. Asahara T, Murohara T, Sullivan A, Silver M, Isner JM, et al. (1997) Isolation of putative progenitor endothelial cells for angiogenesis. *Science* 275(5302): 964-967.
25. Tateishi-Yuyama E, Matsubara H, Murohara T, Ikeda U, Imaizumi T, et al. (2002) Therapeutic angiogenesis for patients with limb ischaemia by autologous transplantation of bone-marrow cells: a pilot study and a randomised controlled trial. *Lancet* 360(9331): 427-435.
26. Stamm C, Westphal B, Kleine HD, Petzsch M, Steinhoff G, et al. (2003) Autologous bone-marrow stem-cell transplantation for myocardial regeneration. *Lancet* 361 (9351): 45-46.
27. Tse HF, Kwong YL, Chan JK, Lo G, Lau CP, et al. (2003) Angiogenesis in ischaemic myocardium by intramyocardial autologous bone marrow mononuclear cell implantation. *Lancet* 361(9351): 47-49.
28. Perin EC, Dohmann HF, Borojevic R, Silva SA, Willerson JT, et al. (2003) Transendocardial, autologous bone marrow cell transplantation for severe, chronic ischemic heart failure. *Circulation* 107(18): 2294-2302.
29. Minamino T, Toko H, Tateno K, Nagai T, Komuro I (2002) Peripheral-blood or bone-marrow mononuclear cells for therapeutic angiogenesis? *Lancet* 360(9350): 2083-2084.
30. Tateno K, Minamino T, Toko H, Akazawa H, Komuro I, et al. (2006) Critical roles of muscle-secreted angiogenic factors in therapeutic neovascularization. *Circ Res* 98(9): 1194-1202.
31. Li Z, Wu JC, Sheikh AY, Kraft D, Wu JC, et al. (2007) Differentiation, survival, and function of embryonic stem cell derived endothelial cells for ischemic heart disease. *Circulation* 116(11 Suppl): 146-154.
32. Yamahara K, Sone M, Itoh H, Yamashita JK, Nakao K, et al. (2008) Augmentation of neovascularization in hindlimb ischemia by combined transplantation of human embryonic stem cells-derived endothelial and mural cells. *PLoS One* 3(2):e1666.
33. Oyamada N, Itoh H, Sone M, Yamahara K, Nakao K, et al. (2008) Transplantation of vascular cells derived from human embryonic stem cells contributes to vascular regeneration after stroke in mice. *J Transl Med* 6(1): 54.
34. Huang NF, Niiyama H, Peter C, De A, Cooke JP, et al. (2010) Embryonic stem cell-derived endothelial cells engraft into the ischemic hindlimb and restore perfusion. *Arterioscler Thromb Vasc Biol* 30(5): 984-991.
35. Rufaihah AJ, Huang NF, Jamé S, Lee JC, Cooke JP, et al. (2011) Endothelial cells derived from human iPSCS increase capillary density and improve perfusion in a mouse model of peripheral arterial disease. *Arterioscler Thromb Vasc Biol* 31(11): e72-79.
36. L'Heureux N, Dusserre N, Konig G, Victor B, McAllister TN, et al. (2006) Human tissue-engineered blood vessels for adult arterial revascularization. *Nat Med* 12(3): 361-365.
37. Roh JD, Sawh-Martinez R, Brennan MP, Jay SM, Breuer CK, et al. (2010) Tissue-engineered vascular grafts transform into mature blood vessels via an inflammation-mediated process of vascular remodeling. *Proc Natl Acad Sci U S A* 107(10): 4669-4674.
38. Margariti A, Winkler B, Karamariti E, Zampetaki A, Xu Q, et al. (2012) Direct reprogramming of fibroblasts into endothelial cells capable of angiogenesis and reendothelialization in tissue-engineered vessels. *Proc Natl Acad Sci U S A* 109(34): 13793-13798.
39. Carvajal-Vergara X, Sevilla A, D'Souza SL, Ang YS, Lemischka IR, et al. (2010) Patient-specific induced pluripotent stem-cell-derived models of LEOPARD syndrome. *Nature* 465(7299): 808-812.
40. Moretti A, Bellin M, Welling A, Jung CB, Laugwitz KL, et al. (2010) Patient-specific induced pluripotent stem-cell models for long-QT syndrome. *N Engl J Med* 363(15): 1397-1409.
41. Itzhaki I, Maizels L, Huber I, Zwi-Dantsis L, Gepstein L, et al. (2011) Modelling the long QT syndrome with induced pluripotent stem cells. *Nature* 471(7337): 225-229.
42. Malan D, Friedrichs S, Fleischmann BK, Sasse P (2011) Cardiomyocytes obtained from induced pluripotent stem cells with long-QT syndrome 3 recapitulate typical disease-specific features in vitro. *Circ Res* 109(8): 841-847.
43. Liu GH, Suzuki K, Qu J, Sancho-Martinez I, Izpisua Belmonte JC, et al. (2011) Targeted gene correction of laminopathy-associated LMNA mutations in patient-specific iPSCs. *Cell Stem Cell* 8(6): 688-694.
44. Soldner F, Laganière J, Cheng AW, Hockemeyer D, Jaenisch R, et al. (2011) Generation of isogenic pluripotent stem cells differing exclusively at two early onset Parkinson point mutations. *Cell* 146(2): 318-331.
45. Koch P, Breuer P, Peitz M, Jungverdorben J, Brüstle O, et al. (2011) Excitation-induced ataxin-3 aggregation in neurons from patients with Machado-Joseph disease. *Nature* 480(7378): 543-546.
46. Sun N, Yazawa M, Liu J, Han L, Wu JC, et al. (2012) Patient-specific induced pluripotent stem cells as a

model for familial dilated cardiomyopathy. *Sci Transl Med* 4(130): 130ra47.

47. Jiang Y, Cowley SA, Siler U, Melguizo D, Armstrong L, et al. (2012) Derivation and functional analysis of patient-specific induced pluripotent stem cells as an in vitro model of chronic granulomatous disease. *Stem Cells* 30(4): 599-611.
48. Wang Y, Zheng CG, Jiang Y, Zhang J, Gao S, et al. (2012) Genetic correction of β-thalassemia patient-specific iPS cells and its use in improving hemoglobin production in irradiated SCID mice. *Cell Res* 22(4): 637-648.
49. Egawa N, Kitaoka S, Tsukita K, Naitoh M, Inoue H, et al. (2012) Drug screening for ALS using patient-specific induced pluripotent stem cells. *Sci Transl Med* 4(145): 145ra104.
50. Quarto N, Li S, Renda A, Longaker MT (2012) Exogenous Activation of BMP-2 Signaling Overcomes TGFβ-Mediated Inhibition of Osteogenesis in Marfan Embryonic Stem Cells and Marfan Patient-Specific Induced Pluripotent Stem Cells. *Stem Cells* 30(12): 2709-2719.
51. An MC, Zhang N, Scott G, Montoro D, Ellerby LM, et al. (2012) Genetic correction of Huntington's disease phenotypes in induced pluripotent stem cells. *Cell Stem Cell* 11(2): 253-263.
52. Lee G, Ramirez CN, Kim H, Zeltner N, Studer L, et al. (2012) Large-scale screening using familial dysautonomia induced pluripotent stem cells identifies compounds that rescue IKBKAP expression. *Nat Biotechnol* 30(12): 1244-1248.
53. Ge X, Ren Y, Bartulos O, Lee MY, Qyang Y, et al. (2012) Modeling supravalvular aortic stenosis syndrome with human induced pluripotent stem cells. *Circulation* 126(14): 1695-1704.

BRIEF REPORT

Intracerebroventricular Administration of C-Type Natriuretic Peptide Suppresses Food Intake via Activation of the Melanocortin System in Mice

Nobuko Yamada-Goto,[1] Goro Katsuura,[1] Ken Ebihara,[1] Megumi Inuzuka,[1] Yukari Ochi,[1] Yui Yamashita,[1] Toru Kusakabe,[1] Akihiro Yasoda,[1] Noriko Satoh-Asahara,[2] Hiroyuki Ariyasu,[1] Kiminori Hosoda,[1] and Kazuwa Nakao[1]

C-type natriuretic peptide (CNP) and its receptor are abundantly distributed in the brain, especially in the arcuate nucleus (ARC) of the hypothalamus associated with regulating energy homeostasis. To elucidate the possible involvement of CNP in energy regulation, we examined the effects of intracerebroventricular administration of CNP on food intake in mice. The intracerebroventricular administration of CNP-22 and CNP-53 significantly suppressed food intake on 4-h refeeding after 48-h fasting. Next, intracerebroventricular administration of CNP-22 and CNP-53 significantly decreased nocturnal food intake. The increment of food intake induced by neuropeptide Y and ghrelin was markedly suppressed by intracerebroventricular administration of CNP-22 and CNP-53. When SHU9119, an antagonist for melanocortin-3 and melanocortin-4 receptors, was coadministered with CNP-53, the suppressive effect of CNP-53 on refeeding after 48-h fasting was significantly attenuated by SHU9119. Immunohistochemical analysis revealed that intracerebroventricular administration of CNP-53 markedly increased the number of c-Fos–positive cells in the ARC, paraventricular nucleus, dorsomedial hypothalamus, ventromedial hypothalamic nucleus, and lateral hypothalamus. In particular, c-Fos–positive cells in the ARC after intracerebroventricular administration of CNP-53 were coexpressed with α-melanocyte–stimulating hormone immunoreactivity. These results indicated that intracerebroventricular administration of CNP induces an anorexigenic action, in part, via activation of the melanocortin system. ***Diabetes* 62:1500–1504, 2013**

C-type natriuretic peptide (CNP) is a member of the natriuretic peptide family and has been demonstrated to be abundantly present in the brain, interestingly in discrete hypothalamic areas, such as the arcuate nucleus (ARC) of the hypothalamus, that play pivotal roles in energy regulation (1–3). Two predominant molecular forms of CNP in the porcine brain were reported to be a 22-residue peptide (CNP-22) and its *N*-terminally elongated 53-residue peptide (CNP-53) (1). Moreover, natriuretic peptide receptor-B (NPR-B), a CNP receptor, is also widely distributed in the brain and is reported to be abundantly expressed in the ARC of the hypothalamus (4,5). These findings indicate the possibility that the brain CNP/NPR-B system may regulate energy homeostasis.

In the current study, we examined the effects of intracerebroventricular administration of CNP on food intake induced by refeeding after fasting and by orexigenic peptides, such as neuropeptide Y (NPY) and ghrelin. Also, we examined the involvement of the melanocortin system in the CNP actions.

RESEARCH DESIGN AND METHODS

Animals and diets. Male C57BL/6J mice (6 weeks old) obtained from Japan SLC (Shizuoka, Japan) were housed in plastic cages in a room kept at a room temperature of 23 ± 1°C and a 12:12-h light–dark cycle (lights turned on at 9:00 A.M.). The mice had ad libitum access to water and food (CE-2; CLEA Japan, Tokyo, Japan). All experiments were performed at 10 weeks of age in accordance with the guidelines established by the Institutional Animal Investigation Committee at Kyoto University and the United States National Institutes of Health Guide for the Care and Use of Laboratory Animals. Every effort was made to optimize comfort and to minimize the use of animals.

Peptides. CNP-22, CNP-53, ghrelin, and NPY were purchased from Peptide Institute (Osaka, Japan). SHU9119 was purchased from Bachem AG (Bubendorf, Switzerland).

Intracerebroventricular injection. Intracerebroventricular injection was performed according to our previous report (6).

Measurement of food intake

Fasting-refeeding. Mice were fasted for 48 h and then refed for 4 h. Water was available ad libitum during the experiments. The intracerebroventricular or intraperitoneal administration of CNP-22 or CNP-53 was performed just before refeeding. Food intake was measured for 4 h of refeeding. At the end of experiments, the hypothalamus was collected for examination of the expressions of mRNA for neuropeptides (7).

Nocturnal food intake. To assess the effect of intracerebroventricular administration of CNP-22 or CNP-53 on nocturnal food intake, peptides were injected intracerebroventricularly 1 h before the beginning of the dark phase. Food intake was measured for 15 h after intracerebroventricular injection. Water was available ad libitum during the experiments.

Food intake induced by NPY and ghrelin. The experiments were performed from 11:00 A.M. to 3:00 P.M. CNP-22 or CNP-53 was intracerebroventricularly administrated just before intracerebroventricular injection of NPY (5 nmol/mouse) or intraperitoneal injection of ghrelin (100 nmol/kg). Food intake was measured for 4 h after peptide injection. In these experiments, food and water were available ad libitum.

PCR. The extraction of mRNA and quantitative real-time RT-PCR were performed according to our previous report (8). Primers for preopiomelanocortin, cocaine and amphetamine-related peptide, *NPY*, agouti gene-related peptide (*AgRP*) and glyceraldehyde 3-phosphate dehydrogenase are shown in Supplementary Table 1.

Immunohistochemistry for c-Fos and α-MSH in the hypothalamus. The immunohistochemical methods and the stereotaxic coordinates for the hypothalamic nuclei were based on our previous report (6). Briefly, mice were anesthetized with pentobarbital at 1 h after intracerebroventricular injection of CNP-53 (1.5 nmol/mouse) and perfused with 50 mL 0.1 mol/L PBS, followed by 50 mL ice-cold 4% paraformaldehyde in 0.1 mol/L PBS. Sections of 30-μm thickness were cut with a cryostat. According to the mouse brain atlas (9), cross-sections were selected in correspondence to −1.70 mm [ARC, lateral hypothalamus (LH), dorsomedial hypothalamus (DMH), ventromedial hypothalamic

From the [1]Department of Medicine and Clinical Science, Kyoto University Graduate School of Medicine, Kyoto, Japan; and the [2]Clinical Research Institute, National Hospital Organization, Kyoto Medical Center, Kyoto, Japan.
Corresponding author: Nobuko Yamada-Goto, nobukito@kuhp.kyoto-u.ac.jp.
Received 31 May 2012 and accepted 7 November 2012.
DOI: 10.2337/db12-0718
This article contains Supplementary Data online at http://diabetes.diabetesjournals.org/lookup/suppl/doi:10.2337/db12-0718/-/DC1.

See accompanying commentary, p. 1379.

nucleus (VMH)] and to −0.82 mm [paraventricular nucleus (PVN)], relative to bregma. For c-Fos and α-melanocyte–stimulating hormone (α-MSH) protein staining, the sections were incubated with antic-Fos rabbit antibody (Ab-5; 1:5,000; Oncogene Science, Cambridge, MA) and antiα-MSH sheep antibody (AB5087; 1:10,000; EMD Millipore, Billerica, MA), respectively. The antibody was detected using the Vectastain ABC Elite kit (PK-6101; Vector Laboratories, Burlingame, CA) and a diaminobenzidine substrate kit (SK-4100; Vector Laboratories) was used for visualization. The second antibodies for fluorescence visualization used were goat anti-rabbit488 (A11008; 1:200; Life Technologies, Carlsbad, CA) for antic-Fos rabbit antibody and goat anti-sheep546 (A21098; 1:200; Life Technologies) for antiα-MSH sheep antibody.

Data analysis. All values are given as the mean ± SEM. Statistical analysis of the data were performed by ANOVA, followed by the Tukey-Kramer test. Statistical significance was defined as $P < 0.05$.

RESULTS

Effects of intracerebroventricular administration of CNP-22 and CNP-53 on food intake at refeeding after fasting. The intracerebroventricular administration of CNP-22 (1.5 and 4.5 nmol/mouse) and CNP-53 (1.5 nmol/mouse) significantly suppressed food intake during 4-h refeeding after 48-h fasting in comparison with data from saline-treated mice (Fig. 1*A*). In this experiment, CNP-53 (1.5 nmol), but not other treatments, induced significant reduction of body weight compared with saline treatment (Supplementary Table 2). The mRNA expressions of pre-opiomelanocortin and cocaine and amphetamine-related peptide significantly decreased, and the mRNA expressions of *NPY* and *AgRP* significantly increased after refeeding compared with control animals (Supplementary Fig. 1). The intracerebroventricular administration of CNP-53 did not influence the mRNA expressions of these neuropeptides in the hypothalamus (Supplementary Fig. 1). Next, the peripheral action of CNP on food intake was examined when a 10-fold greater dose than intracerebroventricular injection of each CNP was intraperitoneally administered. The intraperitoneal administrations of CNP-22 (1.5 μmol/kg) and CNP-53 (0.5 μmol/kg) did not change the food intake during 4-h refeeding after 48-h fasting (Fig. 1*B*), nor were there changes in body weight (Supplementary Table 3).

The intracerebroventricular administrations of CNP-22 (4.5 nmol/mouse) and CNP-53 (1.5 nmol/mouse) at 1 h before the start of the dark phase significantly suppressed nocturnal food intake compared with saline treatment (Fig. 1*C*).

Effect of intracerebroventricular administration of CNP-22 and CNP-53 on NPY-induced and ghrelin-induced food intake. When CNP-22 (4.5 nmol/mouse) and CNP-53 (1.5 nmol/mouse) were concomitantly administered intracerebroventricularly with NPY, they significantly suppressed the food intake induced by NPY compared with that of saline treatment (Fig. 2*A*). When CNP-22 (4.5 nmol/mouse) and CNP-53 (1.5 nmol/mouse) were administered intracerebroventricularly with ghrelin, they significantly suppressed the food intake induced by ghrelin compared with that of saline treatment (Fig. 2*B*).

Effect of melanocortin receptor antagonist, SHU9119, on the anorectic effect of CNP. To examine its involvement in the anorectic effect of CNP, SHU9119 was administered intracerebroventricularly together with CNP-53 (1.5 nmol/mouse). SHU9119 (1 nmol/mouse) significantly attenuated the suppressive action of CNP-53 on the food intake during 4-h refeeding after 48-h fasting, whereas SHU9119 itself significantly enhanced the increase of food intake in comparison with mice administered saline treatment (Fig. 3).

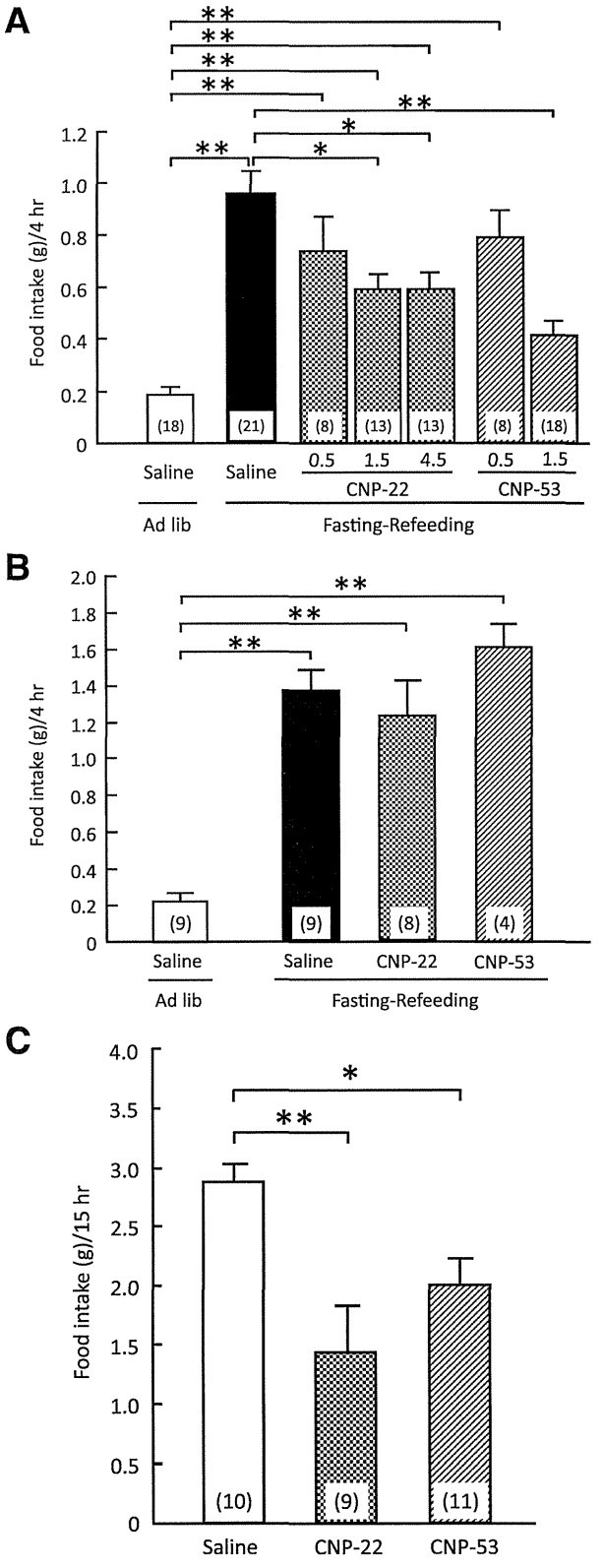

FIG. 1. Effects of CNP on refeeding after fasting. *A*: Effects of intracerebroventricular administration of CNP-22 (0.5, 1.5, and 4.5 nmol/mouse) and CNP-53 (0.5 and 1.5 nmol/mouse) on 4-h refeeding after 48-h fasting in mice. Food intake was observed for 4 h after refeeding. *B*: Effects of intraperitoneal administration of CNP-22 (1.5 μmol/kg) and CNP-53 (0.5 μmol/kg) on 4-h refeeding after 48-h fasting in mice. Food intake was observed for 4 h after refeeding. *C*: Effects of intracerebroventricular administration of CNP-22 (4.5 nmol/mouse) and CNP-53 (1.5 nmol/mouse) on nocturnal food intake in mice. Food intake was observed for 15 h after intracerebroventricular injection. Data represent mean ± SEM. The number of mice is given in parentheses. Significant differences: $^{*}P < 0.05$, $^{**}P < 0.01$.

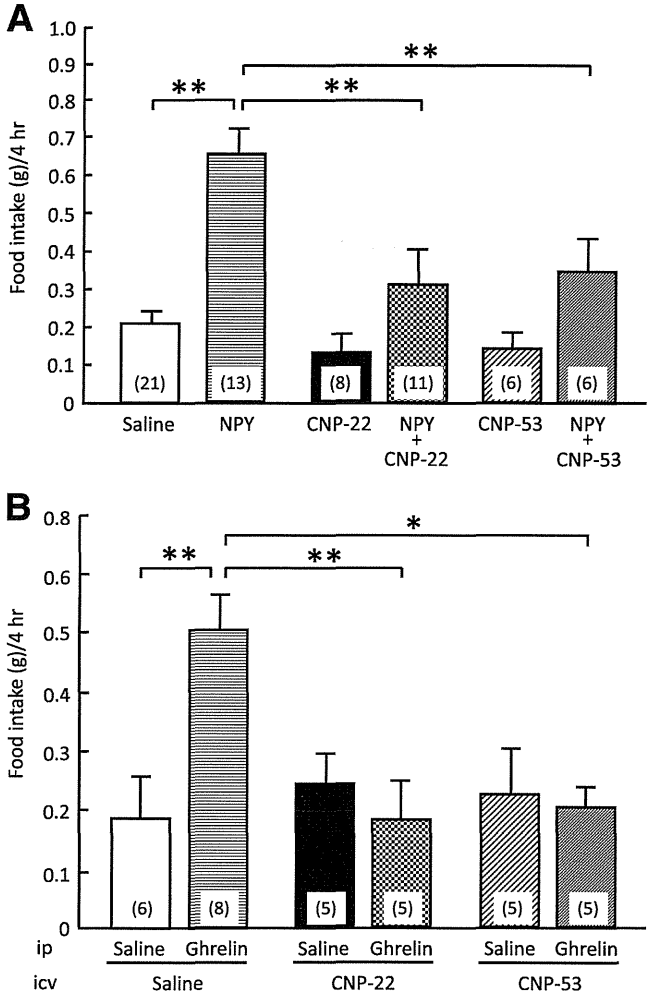

FIG. 2. Effects of CNP-22 and CNP-53 on food intake induced by NPY and ghrelin. *A*: Effects of intracerebroventricular administration of CNP-22 (4.5 nmol/mouse) and CNP-53 (1.5 nmol/mouse) on NPY-induced (5 nmol/mouse, intracerebroventricular) food intake in mice. Food intake was observed for 4 h after coadministration of NPY and CNP. *B*: Effects of intracerebroventricular administration of CNP-22 (4.5 nmol/mouse) and CNP-53 (1.5 nmol/mouse) on ghrelin-induced (100 nmol/kg, intraperitoneal) food intake in mice. Food intake was observed for 4 h after coadministration of ghrelin and CNP. Data represent mean ± SEM. The number of mice is given in parentheses. Significant differences: *$P < 0.05$, **$P < 0.01$.

c-Fos–immunoreactive cells in the hypothalamus after intracerebroventricular administration of CNP. To understand the neuronal pathway involved in the anorectic actions of CNP, the expression of c-Fos, one of the markers of neuronal activation, was monitored by immunohistochemical examination at 1 h after intracerebroventricular injection of CNP-53 (1.5 nmol/mouse). The numbers of c-Fos–immunoreactive cells in the ARC, PVN, and DMH were predominantly increased after intracerebroventricular injection of CNP-53 in comparison with saline treatment (Fig. 4*A*). The c-Fos–positive cells were also moderately increased in the VMH and LH (Fig. 4*A*). Next, we examined whether c-Fos immunoreactivity coexisted with α-MSH–containing cells. In the ARC of saline-treated mice, only a few α-MSH–immunoreactive cells showed weak c-Fos immunoreactivity (Fig. 4*B*). However, c-Fos–immunoreactive cells that increased with intracerebroventricular administration of CNP-53 in the ARC expressed a large amount of α-MSH immunoreactivity (Fig. 4*B*).

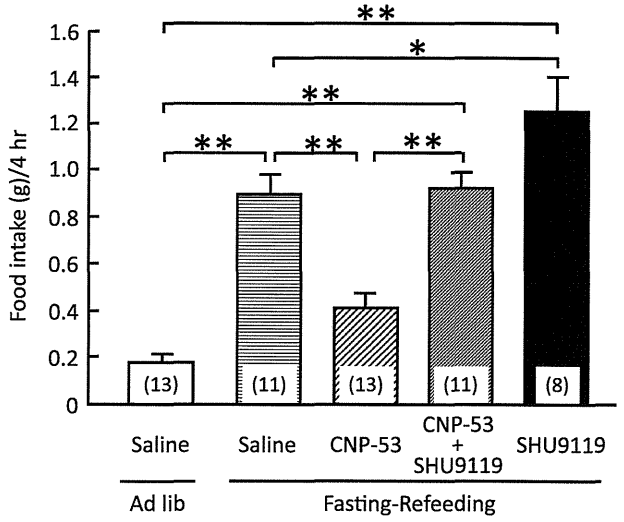

FIG. 3. Effects of intracerebroventricular administration of CNP-53 (1.5 nmol/mouse) and SHU9119 (1 nmol/mouse) on refeeding after 48-h fasting in mice. Food intake was observed for 4 h after refeeding. Data represent mean ± SEM. The number of mice is given in parentheses. Significant differences: *$P < 0.05$, **$P < 0.01$.

DISCUSSION

The current study demonstrated that intracerebroventricular administration of CNP-22 and CNP-53, but not intraperitoneal injection, led to significant reduction of food intake induced by fasting–refeeding. This reduction was inhibited by the melanocortin-3 receptor (MC3R)/melanocortin-4 receptor (MC4R) antagonist SHU9119. In addition, CNP significantly suppressed nocturnal food intake and orexigenic actions induced by NPY and ghrelin. The immunohistochemical study revealed that intracerebroventricular administration of CNP-53 increased the number of c-Fos–expressing cells containing α-MSH in the hypothalamus. These findings indicated that the intracerebroventricular administration of CNP exhibits anorexigenic actions partially via activation of the melanocortin system, although the doses of CNP used in the current study could be pharmacological doses.

The hypothalamus is considered to be an important region in regulating energy homeostasis. In particular, the ARC in the hypothalamus contains both an orexigenic peptide, NPY, and an anorexigenic peptide, α-MSH, and is postulated to be involved in the first-order regulation of food intake. Synthetic MC3R/MC4R agonists, melanotan II, and [Nle^4-D-Phe^7]–α-MSH completely blocked food deprivation–induced increase in food intake as well as the food intake stimulated by intracerebroventricular administration of NPY (10,11). Regarding the reciprocal interactions of α-MSH and NPY, melanocortin neurons in the ARC project to the PVN (12). In the current study, intracerebroventricular administration of CNP significantly suppressed food intake after fasting, which was antagonized by SHU9119. Our results also showed that CNP suppressed NPY-induced food intake. Taken together, these findings indicate that CNP exhibits anorexigenic actions via activation of MC3R/MC4R downstream signaling. However, mRNA expressions of preopiomelanocortin, cocaine and amphetamine-related peptide, *NPY*, and *AgRP* in the hypothalamus after the intracerebroventricular injection of CNP-53 in fasting–refeeding experiment did not change compared with those after saline. The reason for this